Comparative measurements of carbon dioxide fluxes from two nearby towers in a central Amazonian rainforest: The Manaus LBA site

A. C. Araújo,[1] A. D. Nobre,[1] B. Kruijt,[2] J. A. Elbers,[2] R. Dallarosa,[1] P. Stefani,[4] C. von Randow,[5] A. O. Manzi,[5] A. D. Culf,[3] J. H. C. Gash,[3] R. Valentini,[4] and P. Kabat[2]

Received 26 March 2001; revised 25 March 2002; accepted 1 April 2002; published 29 October 2002.

[1] Forests around Manaus have staged the oldest and the longest forest-atmosphere CO_2 exchange studies made anywhere in the Amazon. Since July 1999 the exchange of CO_2, water, and energy, as well as weather variables, have been measured almost continuously over two forests, 11 km apart, in the Cuieiras reserve near Manaus, Brazil. This paper presents the sites and climatology of the region based upon the new data sets. The landscape consists of plateaus dissected by often waterlogged valleys, and the two sites differ in terms of the relative areas of those two landscape components represented in the tower footprints. The radiation and wind climate was similar to both towers. Generally, both the long-wave and short-wave radiation input was less in the wet than in the dry season. The energy balance closure was imperfect (on average 80%) in both towers, with little variation in energy partitioning between the wet and dry seasons; likely a result of anomalously high rainfall in the 1999 dry season. Fluxes of CO_2 also showed little seasonal variation except for a slightly shorter daytime uptake duration and somewhat lower respiratory fluxes in the dry season. The net effect is one of lower daily net ecosystem exchange (NEE) in the dry season. The tower, which has less waterlogged valley areas in its footprint, measured a higher overall CO_2 uptake rate. We found that on first sight, NEE is underestimated during calm nights, as was observed in many other tower sites before. However, a closer inspection of the diurnal variation of CO_2 storage fluxes and NEE suggests that at least part of the nighttime deficits is recovered from either lateral influx of CO_2 from valleys or outgassing of soil storage. Therefore there is a high uncertainty in the magnitude of nocturnal NEE, and consequently preliminary estimates of annual carbon uptake reflecting this range from 1 to 8 T ha^{-1} y^{-1}, with an even higher upper range for the less waterlogged area. The high uptake rates are clearly unsustainable and call for further investigations into the integral carbon balance of Amazon landscapes. *INDEX TERMS:* 0322 Atmospheric Composition and Structure: Constituent sources and sinks; 0315 Atmospheric Composition and Structure: Biosphere/atmosphere interactions; 1615 Global Change: Biogeochemical processes (4805); *KEYWORDS:* tropical forest, eddy flux covariance, Amazon, flux, carbon dioxide, ecological differences

Citation: Araújo, A. C., et al., Comparative measurements of carbon dioxide fluxes from two nearby towers in a central Amazonian rainforest: The Manaus LBA site, *J. Geophys. Res.*, *107*(D20), 8090, doi:10.1029/2001JD000676, 2002.

1. Introduction

[2] The role of forests in the global carbon cycle can only be properly addressed by long term studies monitoring carbon exchange [*Grelle and Lindroth*, 1996]. Long term eddy covariance data serve well in quantifying the effects of seasonality, climate anomalies and phenology on CO_2 exchange, as well as for developing and testing models [*Goulden et al.*, 1996; *Fitzjarrald et al.*, 1990]. Although application of eddy covariance data for the accurate calculation of annually integrated NEE (carbon net ecosystem exchange) is still controversial due to unresolved problems with nighttime fluxes and gap filling [*Aubinet et al.*, 2000], new strategies are starting to address these issues [*Falge et al.*, 2001].

[3] Tropical rainforests are likely to play a prominent role in the global carbon cycle. The rainforest of central Amazonia, with Manaus in its center, is a vast area of dense broadleaf tropical vegetation [*Andreae et al.*, 2002]. Forests around Manaus have staged the oldest and the longest forest-atmosphere CO_2 exchange studies made anywhere in the Amazon, with *Fan et al.* [1990] making the first eddy

[1]Instituto Nacional de Pesquisas da Amazônia, Manaus, Amazonas, Brazil.
[2]Alterra, Wageningen University Research, Wageningen, Netherlands.
[3]Centre for Ecology and Hydrology, Wallingford, UK.
[4]Facoltà di Agraria, Dipartimento DI.S.A.F.RI, Università degli Studi della Tuscia, Viterbo, Italy.
[5]Instituto Nacional de Pesquisas Espaciais, Cachoeira Paulista, Brazil.

0148-0227/02/2001JD000676$09.00

Table 1. Climatologic Parameters Summary for Manaus Region

Parameter	Value	Unit
Top of the atmosphere incoming radiation	30.7–36.7	M J m^{-2} day^{-1}
Average surface incoming radiation range	$16_{(March)}-18_{(Aug.)}$	M J m^{-2} day^{-1}
Average temperature range	$25.8°_{(April)}-27.9°_{(Sept.)}$	degree Celsius
Precipitation	$2{,}431_{(Duke\ reserve)}$	mm $year^{-1}$
Precipitation range	$95_{(Aug.)}-304_{(March)}$	mm $month^{-1}$
Wetter $period_{[convective\ rainfall]}$	$5_{(Nov.\ to\ March)}$	months
Drier period	$5_{(May\ to\ Sept.)}$	months
Transition periods	$1_{(April)}$; $1_{(Oct.)}$	month
Predominant wind direction at C14[a]	$10°-60°_{(Nov.\ to\ March)}$ $90°-130°_{(May\ to\ Sept.)}$	degree azimuth
Climate anomaly	up to $70_{(el\ nino)}$	percent less precipitation

[a] From *Malhi et al.* [1998] for daytime conditions (short wave in >500 W m^{-2}) for period October 1995 through September 1996.

covariance measurements of CO_2 exchange at the Ducke reserve. Before this, uptake rates for CO_2 by photosynthesis have been estimated indirectly using variations in CO_2 concentration observed within and above the tropical forest canopy [*Fan et al.*, 1990; *Wofsy et al.*, 1988]. More recently, *Malhi et al.* [1998] made measurements of the carbon dioxide and energy fluxes for a year at the Cuieiras reserve. *Grace et al.* [1995] and *Malhi et al.* [1998] presented measurements indicating increasing carbon uptake rates over time for the Amazon basin. It is important to assess whether this trend is a long-term or a short-term periodic phenomenon.

[4] Although superficially rainforests appear very similar throughout the Amazon, the region consists of a number of very distinct climatic subregions and many studies stress the high spatial variability in species composition and physiognomy [*Tuomisto et al.*, 1995]. Also, there are pronounced small-scale differences in geomorphology and soils. The Large-Scale Biosphere-Atmosphere Experiment in Amazonia (LBA) provides for a comparison of carbon uptake rates through tower sites between the major climatic regions, but assessment of small-scale variability is a lower priority. The latter issue is crucial, however, when we are to use individual tower data to scale up and assume them to represent whole subregions. The experiment described here addresses that issue, through the comparison of two adjacent patches of tropical rainforest exposed to the same climate. This design allows us to explore the role of small-scale heterogeneities on the regional biospheric exchanges. The present study analyzes a pair of flux data sets collected in the first year of operation of the Cuieiras dual tower setup.

2. Site

[5] Manaus is at present the westernmost site in the LBA east-west transect (see map at http://lba.cptec.inpe.br/lba/). With its shorter dry season, Manaus is in sharp contrast to Santarém, the nearest neighboring LBA site. Being more than 1600 km from the Atlantic, there is no direct oceanic influence on the climate of Manaus, such as there is in Caxiuanã, the easternmost LBA forest tower flux site along the Amazon river axis. There has been much less deforestation in the Manaus region in comparison to the LBA sites around Ji-Paraná in Rondonia. The prevailing northeasterly winds blow over vast expanses of undisturbed rainforest before reaching the site. To avoid the expanding city of Manaus, the LBA site was installed in the Cuieiras reserve of the Instituto Nacional de Pesquisas da Amazonia (INPA). The Cuieiras reserve has an area of 22,735 ha and is located about 60 km north of Manaus, embedded in a vast area of pristine rainforest [*Andreae et al.*, 2002]. It is accessed via ZF-2, an unpaved road running west from the main BR-174 Manaus-to-Caracas highway.

[6] The experiment has two micrometeorological towers 11 km apart. The first tower, known as C14 (formerly as "ZF2"), was built in 1979 and has been used in previous energy, water and carbon exchange studies [*Culf et al.*, 1999; *Malhi et al.*, 1998; *Kruijt et al.*, 2000]. It is a 6.0 m square-section steel tower, 41.5 m tall, on a large flat plateau (2°35″21.08″ S, 60°06″53.63″ W, 140 m asl). Because it is larger than those commonly used for eddy covariance measurements, there is the possibility that the aerodynamic flow-distortion might affect the measurements. However, *Malhi et al.* [1998] concluded that these effects are small. The second tower, known as K34, was erected in1999. It is a 1.5 m × 2.5 m-section aluminum tower, 50 m tall, on a medium sized plateau (2°36″32.67″ S, 60°12″33.48″ W, 130 m asl). A selective logging experiment study was conducted near the center of the reserve, with 12 ha being investigated in 1987/88 and 4 ha in 1993. The extraction of trees represented on average 50 m^3 ha^{-1} [*Higuchi et al.*, 1997], or ∼15% of the average dry biomass for the area. The resultant small disturbance is located ∼8 km from either tower and hence represents a small area (only 0.05%) on the outer edges of the footprint of the towers.

2.1. Weather and Climate

[7] There are three macro and mesoscale mechanisms which determine rainfall in the region: diurnal convection resulting from surface heating; instability lines propagating from N-NE inland, from the Atlantic coast; and mesoscale and large-scale aggregated convection associated with frontal systems from S-SE [*Fisch et al.*, 1998]. Selected climatologic variables are presented in Table 1. In this area El Niño (97/98) and La Niña (98/99), both multiyear recurrent phenomena, produce drier and wetter climate anomalies respectively. Localized wind gusts in strong storms can produce wind throw of trees in so-called blowdowns [*Nelson et al.*, 1994], which can be of significance to short-term small-scale carbon turnover and even sometimes cause damage to towers.

2.2. Terrain, Soil, and Vegetation

[8] There is very little large-scale relief in this region, but at a smaller scale the dense drainage network has formed a pattern of plateaus and valleys with a maximum height

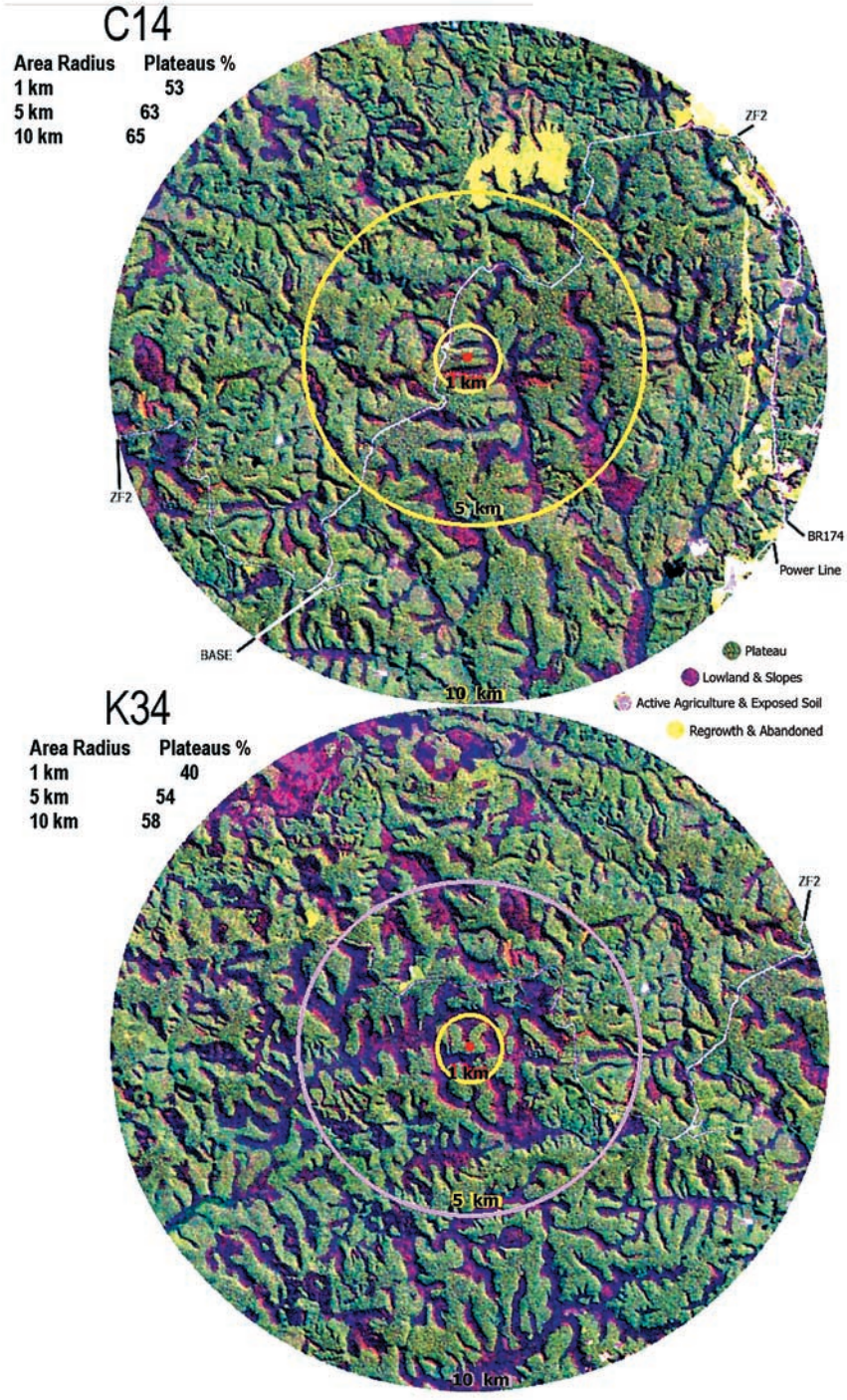

Figure 1. Landsat images of terrain for K34 and C14 towers. Nonplateau pixels were masked and counted. Within the masked area, K34 has more of U-shaped valleys that present larger waterlogged areas in its bottom, whereas C14 has more of V-shaped valleys, with much less waterlogged vegetation.

difference of about 60 m. This undulating landscape can be clearly seen in the satellite images shown in Figure 1. We have visually masked the relief in the images and counted pixels for plateaus and lowlands within concentric areas 1 km, 5 km and 10 km radius from the towers. The plateaus at C14 occupy a larger area (53%, 63% and 65% respectively) than the plateaus at K34 (40%, 54% and 58%) [*Araújo et al.*, 2000]. Thus K34 has significantly more area with lowland-waterlogged vegetation than C14. The tertiary sediments of the Barreiras formation are covered mostly by clayey Oxisols on the plateaus and sandy Spodosols on the valley bottoms. The botanical families Caesalpiniaceae, Vochysiaceae, Euphorbiaceae, Clusiaceae, Sapotaceae, Myristicaceae, Rutaceae, Malphighiaceae, and Anacardiaceae are

Table 2. List of Measurements, Instruments, and Measurement Heights for the Automatic Weather Station Installed at the K34 Tower and for Eddy Correlation Instrumentation Installed on K34 and C14 Towers

Measurement	Instrument Used	Height, m/Depth, m
Shortwave in and out	Kipp & Zonen Pyranometer CM 21	44.60
Longwave in and out	Kipp & Zonen Pyrgeometer CG 1	44.60
PAR	LI-COR LI-190SZ quantum sensor	51.6
Relative humidity	Vaisala HMP35A	51.1
Soil heat flux	Hukseflux SH1	0.01
Wind direction	Vector W200P	51.45
Wind speed vertical profile	Vector A100R	51.9; 42.5; 35.3; 28.0
Rainfall	EM ARG-100	51.35
Surface temperature	Heimann KT15 infrared sensor	50.40
Air pressure	Vaisala PTB100A	32.45
Longwave in and out temperature	PT100	44.60
Air temperature vertical profile	PT100	51.1; 42.5; 35.5; 28.0; 15.6; 5.2
CO_2 concentration vertical profile	PP Systems CIRAS SC IRGA	53.1; 35.3; 28.0; 15.6; 5.2; 0.5
H_2O concentration vertical profile	PP Systems CIRAS SC IRGA	53.1; 35.3; 28.0; 15.6; 5.2; 0.5
Soil temperature profile	IMAG-DLO MCM101	0.01; 0.05; 0.2; 0.4; 1.0
Soil moisture profile	IMAG-DLO MCM101	0.01; 0.05; 0.2; 0.4; 1.0
CO_2 concentration	IRGA LI-COR 6262 closed-path	53,1 and 46,1[a]
H_2O concentration	IRGA LI-COR 6262 closed-path	53,1 and 46,1[a]
U, V and W wind vectors speed	solent three-axis ultrasonic anemometer	53,1 and 46,1[a]

[a] C14 tower; all other instruments are installed in K34 tower.

most frequently found [*Jardim and Hosokawa*, 1987]. An indication of the vertical leaf area distribution along with a characterization of the in-canopy turbulent mixing regime at the C14 tower is given by *Kruijt et al.* [2000].

3. Instruments and Measurements

3.1. Eddy Flux Covariance

3.1.1. Air Motion

[9] Two Solent 1012R2 three-axis ultrasonic anemometers (Gill Instruments, Lymington, UK) measured fluctuating wind components. Rainfall affects neither the instrument (waterproof and with hydrophobic transducers), nor its measurements (onboard high-frequency spurious-signal filtering). Simultaneous measurements with analogue sensors are digitized and appended to the turbulence signals through a built-in 5-channel analogue to digital (A/D) converter with an input range of 0–5 V and resolution of 11 bits. Wind components and sound velocity are output by the sonic at 21 Hz, but the channels of the A/D converter are sampled at only 10 Hz [*Moncrieff et al.*, 1997; *Grelle and Lindroth*, 1996; *Aubinet et al.*, 2000]. In order to protect the signals from ground loop effects the inputs of the ultrasonic anemometer and the outputs of the connected instruments have been electronically separated using instrumentation amplifiers [*Elbers*, 1998]. Sonics and tube inlets (see next section) were extended 5 m and 3 m above the top of the C14 and K34 towers, respectively. C14 sonic was placed on a lateral boom offset 3 m from the tower. Both instruments faced the predominant wind (NE).

3.1.2. H_2O and CO_2 Concentration

[10] Concentrations of H_2O and CO_2 were measured by LI-6262 infrared gas analyzers (LI-COR, Lincoln, Nebraska, USA) . The quoted response time (time needed to respond to 95% of a one-time step change in gas concentration) is 0.1 s. The LI-6262 is a differential analyzer that compares the absorption of infrared light by water and CO_2 in two chambers within the optical bench [*Moncrieff et al.*, 1997; *Grelle and Lindroth*, 1996; *Aubinet et al.*, 2000]. The analyzers were used in absolute mode, i.e. the reference chamber was flushed with pure nitrogen gas from a cylinder and maintaining a flow rate of about 20 ml min^{-1}. The N_2 was brought to the analyzer from the bottom of the tower through stainless steel tubing with a diameter of 4 mm. In this setup the calculated mixing ratios of H_2O and CO_2 (corrected for analyzer cell temperature, pressure, cross sensitivity and band broadening) were output as analog signals requiring no further corrections to be made to the raw signals. This analog output was fed to the ultrasonic anemometer A/D converter. The IRGA was recalibrated at intervals of about 2 months. CO_2 in artificial air from a calibrated cylinder was used for CO_2 span calibration, and for H_2O span calibration, a LI-COR LI-610 dew point generator was used. Very little drift in analyzer calibration was noted over a diurnal cycle, in accordance with *Aubinet et al.* [2000]. When the slope drift is very low, the impact of the calibration interval on the fluxes is limited.

[11] The air was brought to the gas analyzer through 1 meter of stainless steel tubing at the intake preceded by ~4.48 m and ~7.48 m of Teflon tubing for K34 and C14 towers, respectively. The inner diameter of the tube was 4 mm. The intake was placed next to the measuring volume of the sonics at a distance of 20 cm for K34 and underneath the measuring volume at C14. The air was sucked in by a small membrane air pump (KNF, Neuberger, Germany) at a flow rate of ~7.6 L min^{-1} to prevent condensation and ensure turbulent flow inside the tube [*Aubinet et al.*, 2000]. The IRGA was placed in a cabinet on the tower, at the uppermost tower level, below the sonic. The concentrations calculated by the analyzer were corrected for the effect of the pressure drop within the analyzer's sample chamber by a pressure transducer LI-COR 6262-03. To prevent dust ingress into the sample tubing air filters were used (ACRO 50 PTFE 1 μm; Gelman, Ann Arbor, Michigan, USA). These filters were replaced frequently.

3.1.3. Data Acquisition and Software

[12] Digital data were offloaded at 10.4 Hz from the sonic and stored on a PCMCIA card using a low-power palmtop computer and the DOS program EDDYLOG developed at Alterra (the Dutch partner's institute). The stored raw data

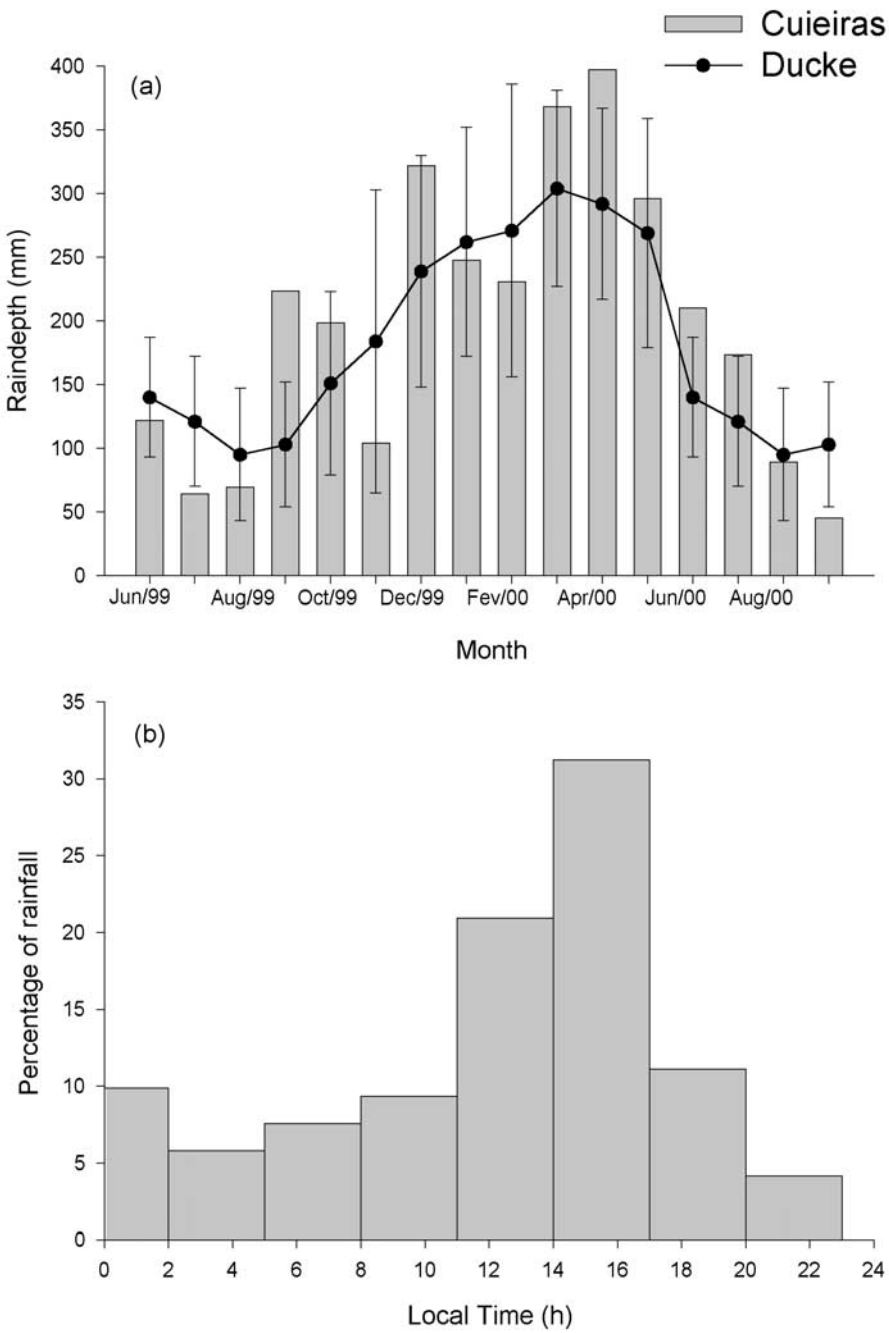

Figure 2. Long-term rainfall (a) from the Ducke reserve compared with the data from Cuieiras reserve at K34 tower since July 1999 until September 2000, and (b) day averaged hourly distribution of rainfall for K34 tower during the same period. The error bars represent standard deviations.

were processed using the eddy correlation data processing software EDDYWSC. It has been written in FORTRAN and it can be adapted to a number of different hardware configurations and software options. The program calculates half-hourly fluxes, means and variances and applies the necessary corrections. Compensation for the time delay down the gas sample tube is performed dynamically by searching the lag at which the cross-correlation between vertical wind and scalar signal is maximum, within preset limits. The raw signals were detrended using a one-sided autoregressive running mean with a time constant of 800 s, after which covariances were determined from the deviations from that running mean. Full 3-D coordinate rotations were applied a posteriori on a variances and covariances [*McMillen*, 1988]. Corrections were applied to the fluxes for loss of covariance at high and low frequencies [*Moore*, 1986]. Generally, the high-frequency corrections are very small, as a result of the large measurement height and low wind speed, but for the same reasons the corrections at the low end could be substantial, although never excessive thanks to the relatively long time constant of the running mean. The eddy correlation systems have a low power

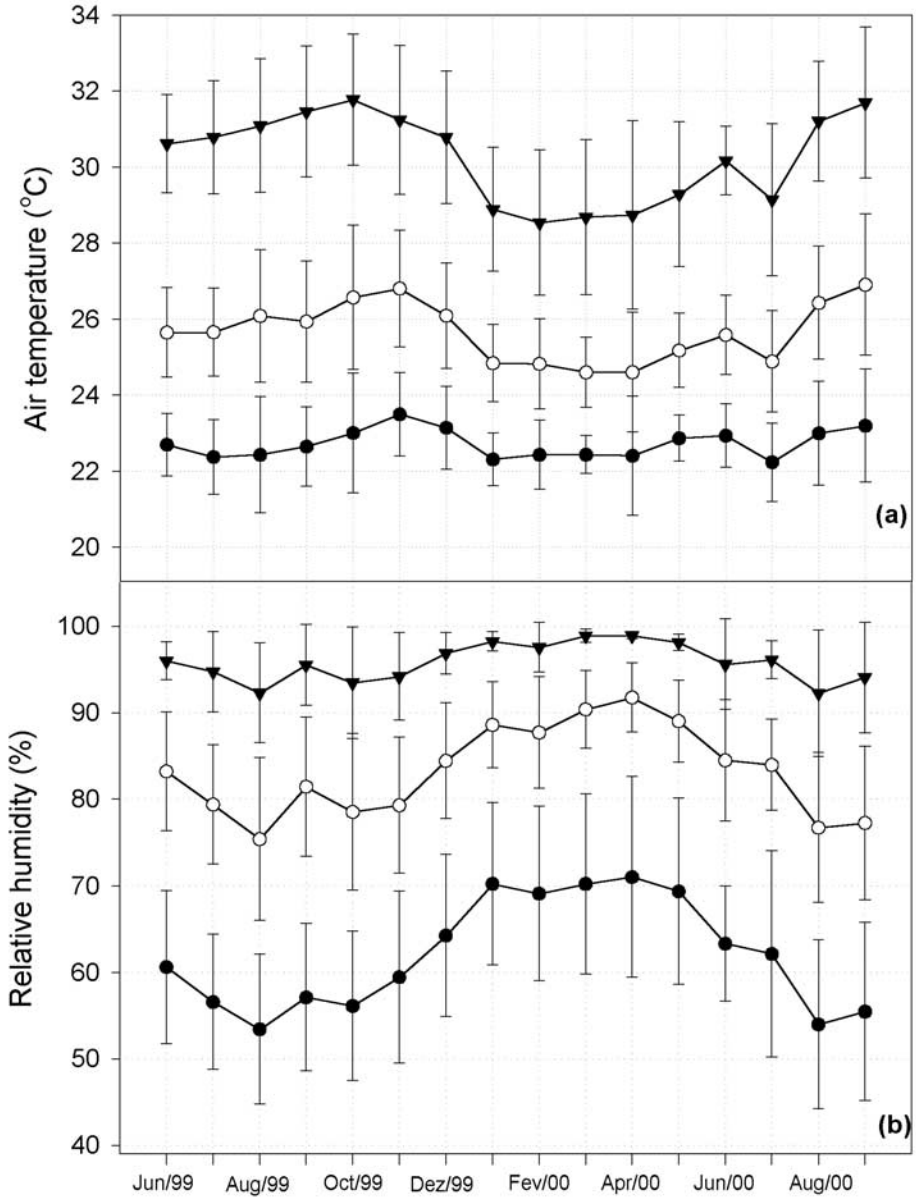

Figure 3. Monthly variation of two weather variables during the 1999/2000 period for the K34 tower: (a) average and average minimum and maximum air temperature; and (b) average and average minimum and maximum relative humidity.

consumption (~50 W) and were powered by batteries maintained by solar panels allowing long-term continuous measurements. Measurements with the eddy correlation systems started in July and September of 1999 at K34 and C14 towers, respectively.

3.2. H_2O and CO_2 Vertical Profiles

[13] At the K34 tower CO_2 and H_2O concentrations were measured at six heights (0.5, 5.0, 15.0, 28.0, 35.0, 53.4 m) using a CIRAS-SC infrared gas analyzer (PP SYSTEMS, UK). This analyzer, with a stated precision of about 0.1 ppm, performs an auto-zero every half hour and thus has little long-term drift. The air was brought to the gas analyzer through low-density polyethylene tubing (until August 2000) and HDPE-lined Dekabon tubing (since September 2000), with an inner diameter of 4 mm. The topmost sample came from the outlet of the eddy correlation system, permitting consistency checks between the two instruments. The profile system sampled each height for 5 min, cycling through the entire profile every half hour using a set of remotely controlled solenoid valves together with a small membrane air pump (KNF, Neuberger, Germany). At each height, there was enough time to flush the tubing of residual air before sampling with the analyzer. The data were logged on a Campbell CR-10 (Campbell Scientific, UK).

3.3. Meteorological Variables

[14] At the K34 tower measurements of weather variables were logged on a Campbell CR-10 (Campbell Scientific, UK) data logger with a sampling interval of 30 sec and

stored as 30 min averages. This unit was also used to log the CO_2 and H_2O concentrations of the vertical profile. A full list of measurements and instruments used is given in Table 2. The automatic weather station started operation in June 1999. Short sets of soil moisture and soil temperature measurements are available but the instruments suffered from frequent failure and were ultimately destroyed by a lightning strike.

4. Results and Discussion

4.1. Data Availability

[15] In general, the instrumentation at this site performed well. Automatic weather station instrument failures caused loss of 24 full days since 15 June 1999 (the first measurement) until 30 September 2000 (n = 473; data coverage of 94.92%). For the flux measurements the instrument failures caused the loss of 42 full days at the K34 tower since 19 July 1999 (the first measurement) until 30 September 2000 (n = 439; data coverage of 90.43%), and 50 full days at the C14 tower since 11 October 1999 (the first measurement) until 30 September 2000 (n = 356; data coverage of 85.96%). For the storage measurements instrument failures caused the loss of 24 full days since 31 August 1999 (the first measurement) until 30 September 2000 (n = 397; data coverage of 93.95%). Most of the failures on the K34 tower were due to lightning strikes, and on the C14 tower due to mechanical problems on the data storage media. The gaps in the eddy correlation data are distributed relatively evenly throughout the year, and are practically noncoincident between the two towers. That translates in an almost continuous availability of raw data for the Cuieiras reserve during the period of this study. Nevertheless, the first year of data analyzed here as the beginning of a long-term time series is still insufficient for the definition of a long-term trend.

4.2. Water and Energy

4.2.1. Rainfall, Temperature, and Wind Speeds

[16] Total rainfall for July 1999 to June 2000 was 2730 mm, larger than the long-term mean value of 2431 mm (sd 366 mm) recorded at Ducke Reserve for the period 1965 to 1993 (Figure 2a). The rainfall in September of 1999 was more than double the average rainfall for the month, an effect that can be attributed to ''La Niña'' which typically leads to high rainfall in the northern part of central Amazonia [*Nobre et al.*, 2000]. Even in the driest months of the year (July–September), rainfall at this site was frequent with more than 1 mm falling on 30% of the days. In the wettest months 75% of days have rainfall greater than 1 mm. Average hourly distribution of rainfall throughout the day is illustrated in Figure 2b. For the 1999 to 2000 period considered in the present study, about 50% of the rainfall fell between 1100 and 1700 local time. The most common storm length was less than 30 min with the mean length being 2 h. There was very little month-to-month variation of air temperatures at the site as shown in Figure 3a, with average monthly values only varying between 24.6 and 26.9°C. Daily maximum temperatures reached average values of 31.8°C during October 1999 and September 2000. Daily minimum temperatures were 22.7°C on average with little seasonal variation. Daily average relative humidity varies from minimum values of 75% during the relatively dry August 1999 to 92% during the height of the rainy season in April 2000 (Figure 3b). The daily range is large with the air being saturated on most nights, but with daytime values dropping to as low as 50% during the driest months of the year. Daily mean vapor pressure deficit (VPD) behavior in the period (Figure 4) indicated pronounced seasonality of atmospheric evapotranspiration forc-

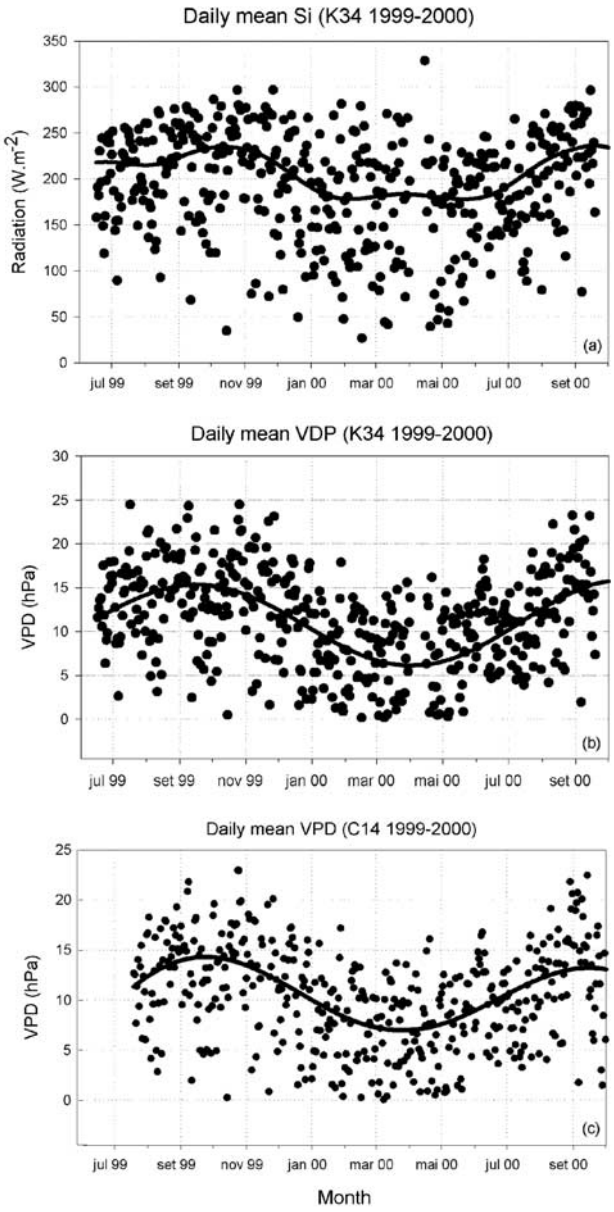

Figure 4. Seasonal variations of the incoming solar radiation and water vapor pressure deficit during the 1999/2000 period: (a) daily average values of incoming solar radiation at K34 tower; daily (10–14 h) average values of water vapour pressure deficit at K34 (b) and C14 (c) towers, respectively. The water vapor pressure deficit from K34 was calculated from air relative humidity and air temperature, and for C14 was calculated from dry and wet bulb air temperature. Solid lines represent fitted curves to the data.

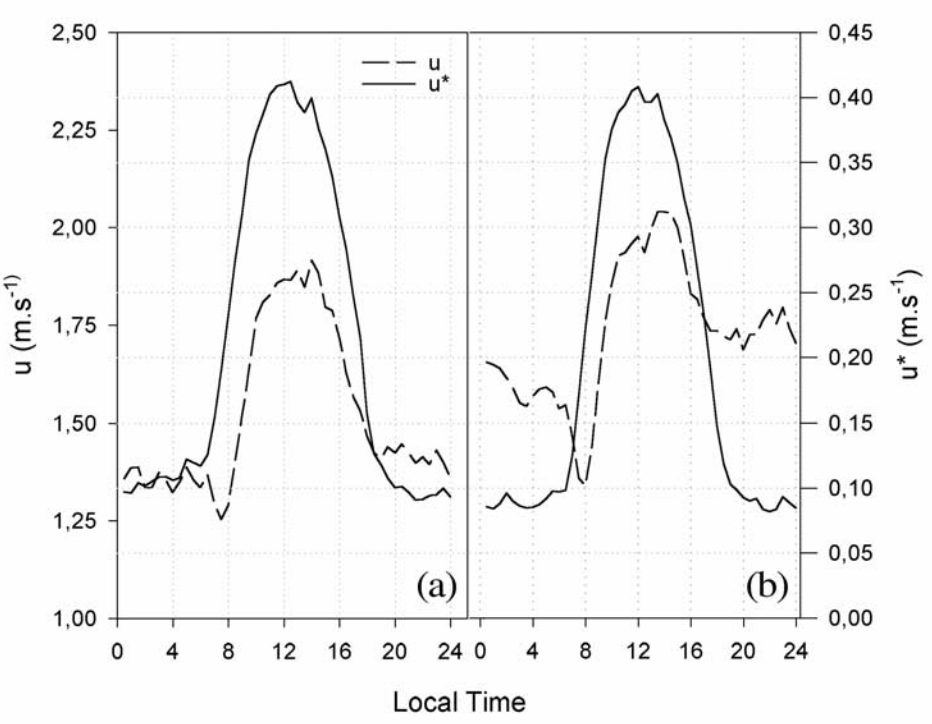

Figure 5. Mean diurnal cycle of the wind speed (U) and friction velocity (u*) at (a) C14 tower (late September 1999 to September 2000) and (b) K34 tower (late July 1999 to September 2000). Both variables measured by sonic anemometers.

ing, very similar for both towers. Water excess in the period driven by La Niña did not suppress the seasonal effect on VPD.

[17] The mean daily wind speeds recorded by the sonic anemometers at the top of the towers were 1.9 m s^{-1} (±0.9 m s^{-1}) for K34 and 1.5 m s^{-1} (±0.7 m s^{-1}) for C14, both quite constant throughout the year. Comparative analysis of the hourly mean wind speeds (U) and hourly mean friction velocities (u*, Figure 5) show differences in U explained by the difference in measurement heights. Similarities between the towers in u*, with a matched variation during daytime, and nighttime values always below 0.15 m s^{-1}, give a good measure of comparability for fluxes. Difference of mean friction velocities between the towers was less than 5%. There are dips in wind speed in early morning between 600 and 800 h, immediately before flushing-out of CO_2-enriched air happens, as will be shown below. Wind roses for daytime and nighttime indicated that east is the predominant wind direction during the day, although all directions do occur (wind roses not shown here). There is little difference between the daytime and nighttime wind roses except for a slight increase in the proportion of northerly and southeasterly wind during the night and a reduction in the frequency of the strongest winds. Southerly winds, which could carry pollution from the city of Manaus to the site [*Culf et al.*, 1999], are among the least common wind directions.

4.2.2. Radiation

[18] The seasonal variation in cloud cover affected the fluxes of both longwave and shortwave radiation. Figure 6a shows the mean diurnal trends of longwave, upward and downward radiation for the wet and dry seasons. While downward fluxes of longwave radiation (Li) are similar in daytime for both seasons, they become relatively larger in nighttime during the wet season. This most likely results from nighttime cloudiness. Upward fluxes (Lo), are similar in both seasons during the night, but show higher daytime values in the dry season, probably due to higher surface temperatures. As a result of both these effects the difference between emitted and received longwave radiation (the Ln balance), becomes more negative in the dry season (Figure 6b).

[19] The frequency of clear and cloudy days has been assessed by examining the ratio of daily totals of incoming solar radiation to the incoming radiation at the top of the atmosphere. Figure 7a shows the frequency distribution of this ratio for 1999 to 2000. For 47% of the days the ratio is greater than 0.5. The ratio tends to be low more often during the wet season. The degree of cloudiness, in the absence of a measurement of diffuse radiation, is of direct relevance to the carbon balance. It has been shown that diffuse radiation, proportionally higher under cloudy conditions, penetrates canopies and leaves more efficiently, leading to relatively higher photosynthetic capacities. Daily cycles representing averaged days of incident (Si), net (Rn), reflected (So) and longwave net radiation (Ln), are presented in Figures 7b (dry season) and 7c (wet season). There appears to be a tight correspondence between Rn and Si, similar to reports by *Malhi et al.* [2002] and *Dallarosa and Clarke* [2000].

[20] The seasonal variations in the radiation components Si, So, Rn and Ln, are shown as monthly averages in Figure 8a. The seasonal variation in albedo is shown in Figure 8b. As first demonstrated by *Culf et al.* [1995], there is a small seasonal variation, with higher values during the dry season. The cause of this variation in albedo, which has been

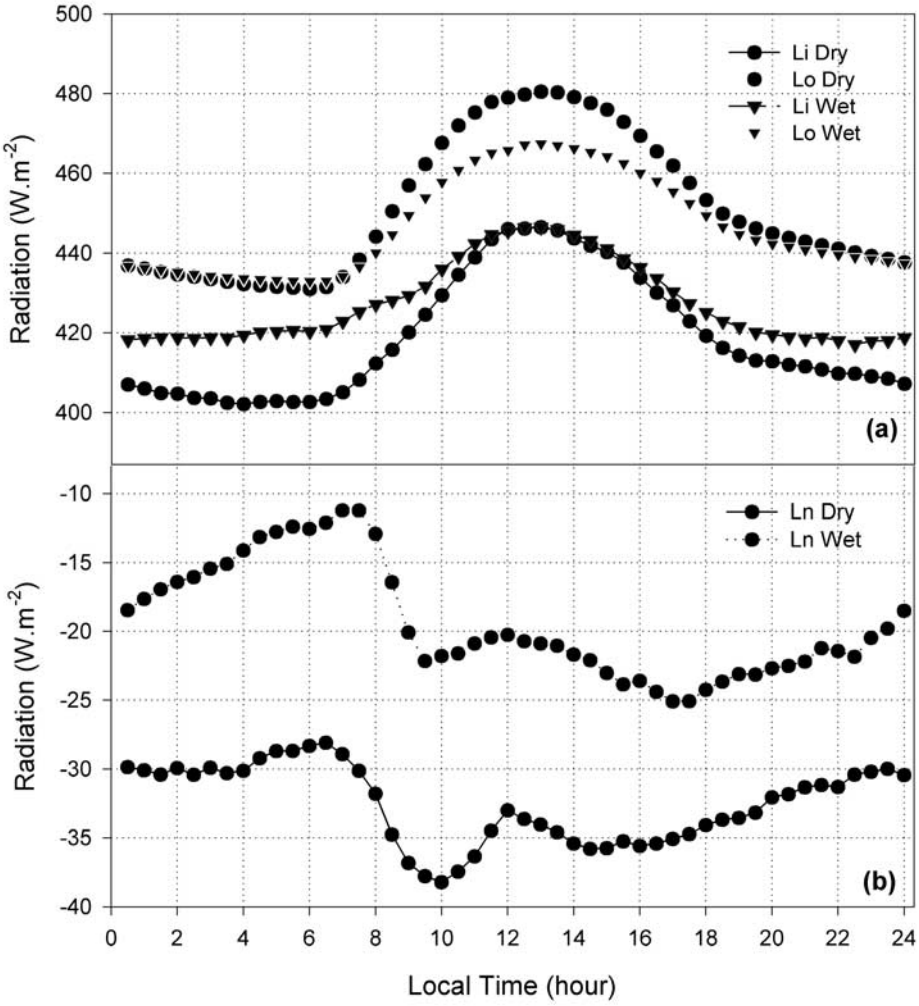

Figure 6. Mean diurnal cycle of: (a) Longwave radiation budget at K34 tower on dry season (mid-July to November 1999) and on wet season (December 1999 to May 2000), and (b) net longwave radiation at K34 tower during the same period.

observed at several sites in Amazonia, has not been definitively established, but it is likely to depend on the physiological or phenological state of the vegetation.

4.2.3. Turbulent Fluxes

[21] The energy balance ratio ((H + LE)/Rn) for the two towers (Figure 9), on average 80% (r^2 = 0.93), although poor, is not smaller than values that are usually reported for most forests [*Aubinet et al.*, 2000]. Seasonally separated H and LE fluxes plotted against Rn are shown in Figures 10 and 11, respectively. In contrast to the observations by *Malhi et al.* [1998, 2002] made in a normal year (95/96) at C14, energy partitioning for both towers in this La Niña year had minimal variation during different seasons. Availability of water during the dry seasons might be the reason for the smaller temporal change in energy partitioning. *Culf et al.* [2000] carried out a study with the same data showing partitioning of net radiation into H and LE fluxes immediately following a rainfall event. They showed that LE increases progressively each day after the event, but falls after the fifth day when H, which was stable to that point, starts to increase. Such results emphasize the importance of radiation and water availability to the H and LE fluxes, and, consequently, to the energy balance closure.

4.3. Footprint Analysis

[22] The horizontal extent of the forest area that contributes 80% of all fluxes was estimated by applying the algorithm proposed by *Schuepp et al.* [1990] to each data record. In this algorithm the 80% cumulative contribution distance increases with measurement height and with increasing stability, and decreases with surface roughness and increasingly unstable conditions. These distances were plotted against the associated wind direction on a polar plot and the symbols coded according to the associated sensible heat fluxes. This creates a two-dimensional picture of the shape of the area ''seen'' by the towers over time.

[23] Figure 12 shows these footprint areas for unstable conditions (and $u^* > 0.2$) for both towers, overlaid onto a Landsat TM image (RGB channels 3, 4, 5) of the Cuieiras reserve. For most unstable conditions the footprints of these towers have little overlap, so that their CO_2 exchange measurements are reasonably independent, and representa-

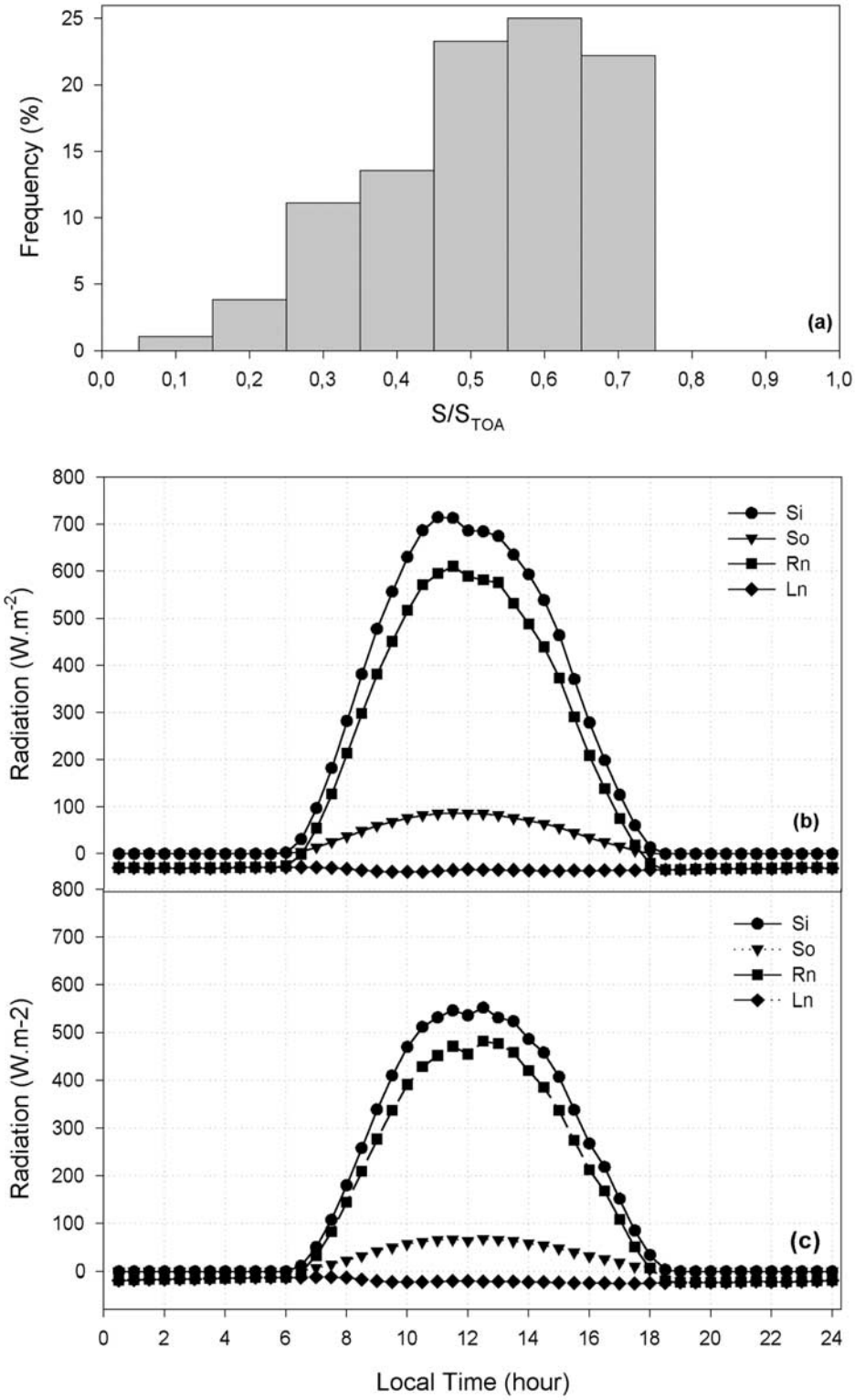

Figure 7. (a) Frequency distribution of cloudiness through the ratio of incoming solar radiation over surface to solar radiation on TOA at K34 tower (July 1999 until September 2000); (b) mean diurnal cycle of radiation budget at K34 tower, dry season (mid-July to November 1999); and (c) wet season (December 1999 to May 2000).

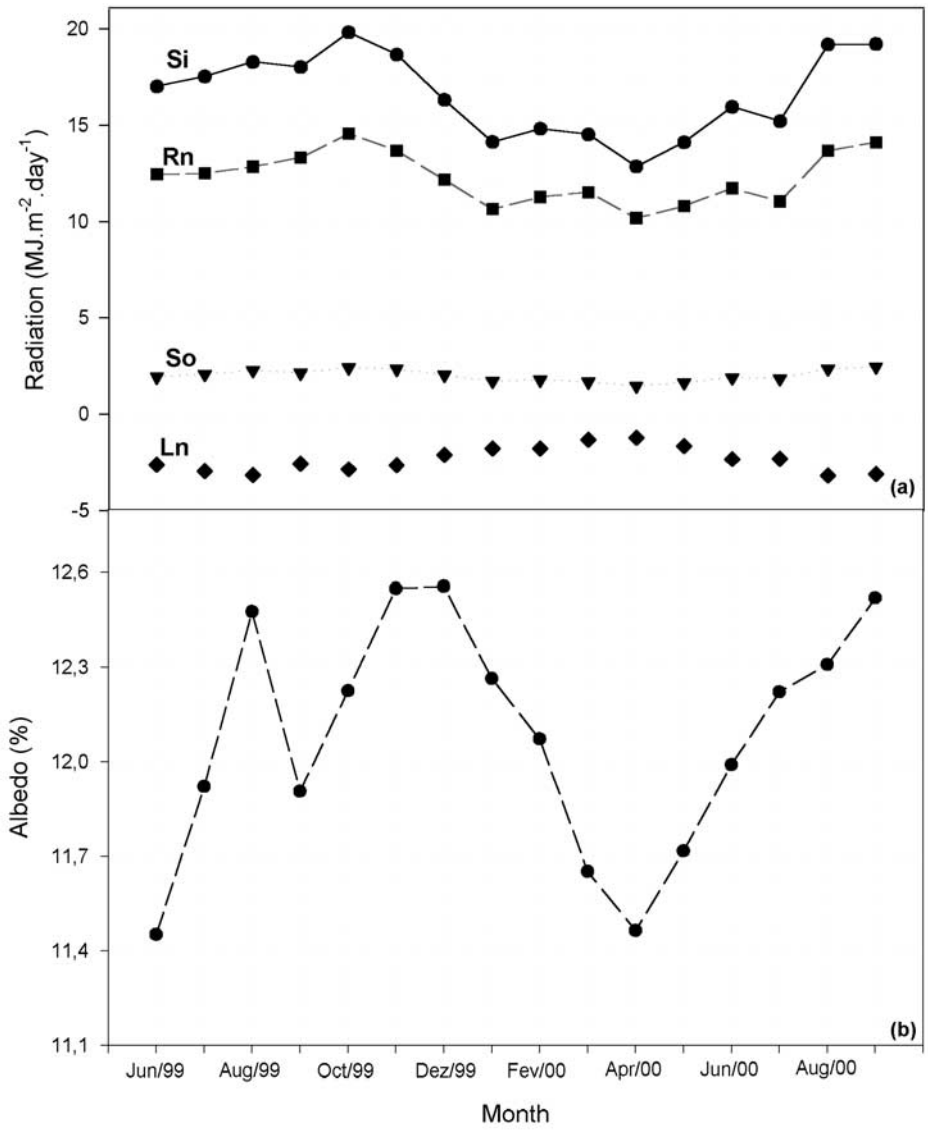

Figure 8. Radiation at the K34 tower during the 1999/2000 period. (a) Monthly average values of radiation budget and (b) monthly average values of albedo.

tive of the ensemble of vegetation types covered by the footprint. Although the measurement height at the C14 tower was lower than that at the K34 tower, the calculated footprint areas of both towers are similar in size and extent. Typically, daytime fluxes are representative of a $2-3$ km^2 area around the towers, although a smaller proportion of fluxes originates from an area as large as $70-80$ km^2. The footprint analysis does not indicate a preferential direction of the source/sink location, although the scatter may obscure the predominance of easterly winds. Summarizing, this analysis supports the assumption that the flux data measured at these towers are representative for most medium-scale topographical landscape elements in the area, including plateaus, slopes and valley bottoms.

4.4. Carbon Dioxide Fluxes

4.4.1. Seasonal and Spatial Variation of CO_2 Flux

[24] Figure 13 gives an overview of the above-canopy, storage uncorrected CO_2 fluxes in the entire data sets of K34 and C14 up to late 2000. The plots are based on 10-day average diurnal trends plotted along date and time of day. Periods with missing data of 10 days and longer show as dark horizontal lines in the contour plots. The periods of daytime uptake and nighttime emissions are clearly distinguishable. It is also apparent from Figure 13 that there is very little seasonal variation in either site in the daytime maximum or average nighttime values. On closer inspection, however, the graphs show a seasonal variation in length of the period during which the forest takes up carbon. This is unlikely to be related strongly to variation in day length, which is minimal at that latitude, but rather seems to be related to the timing of wet and dry seasons. Shortage of soil water in the dry season coinciding with higher air VPD can trigger early stomata closure, which could explain less photosynthesis in the afternoon, in spite of availability of radiation [*Malhi et al.*, 1998, 2002]. Although the daytime peak uptake rates seem almost constant over the year, there is an apparent variation in the magnitude of emission fluxes

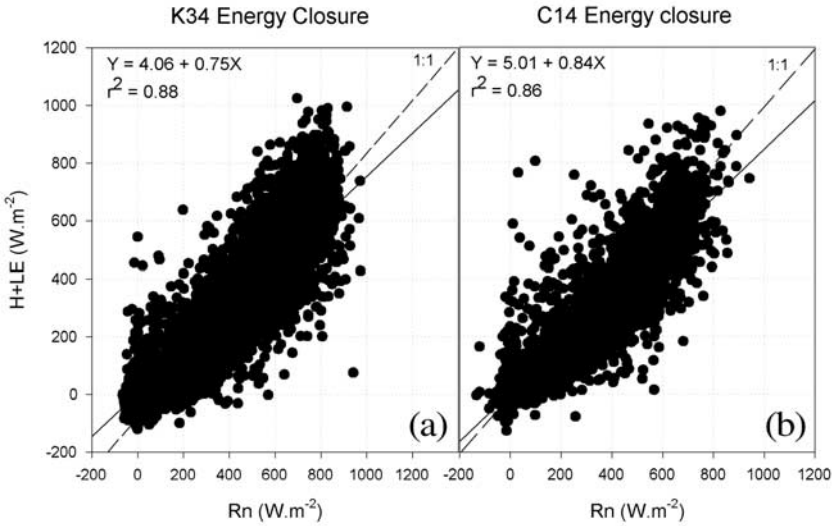

Figure 9. Energy fluxes as a function of net radiation for K34 (a) and C14 (b), respectively. Points for K34 are half-hourly averages from late July 1999 until September 2000 (n = 17454) and for C14 are hourly averages from mid-October 1999 until September 2000 (n = 8522). K34 net radiation was derived from the radiation budget and C14 net radiation was obtained from a net radiometer.

during early morning flush, which are slightly elevated in the dry seasons. These patterns of apparent day length are very similar for both towers, indicating that these physiological responses are controlled by regional meteorological variables rather than being site-specific phenomena. The combined effect of shortened diurnal uptake periods and higher morning emissions leads to a weak seasonal variation in daily total net ecosystem flux. This is shown in Figure 14, where the annual course of average daily totals for both sites is plotted along with a multisine fit [*Kruijt et al.*, 2002] to

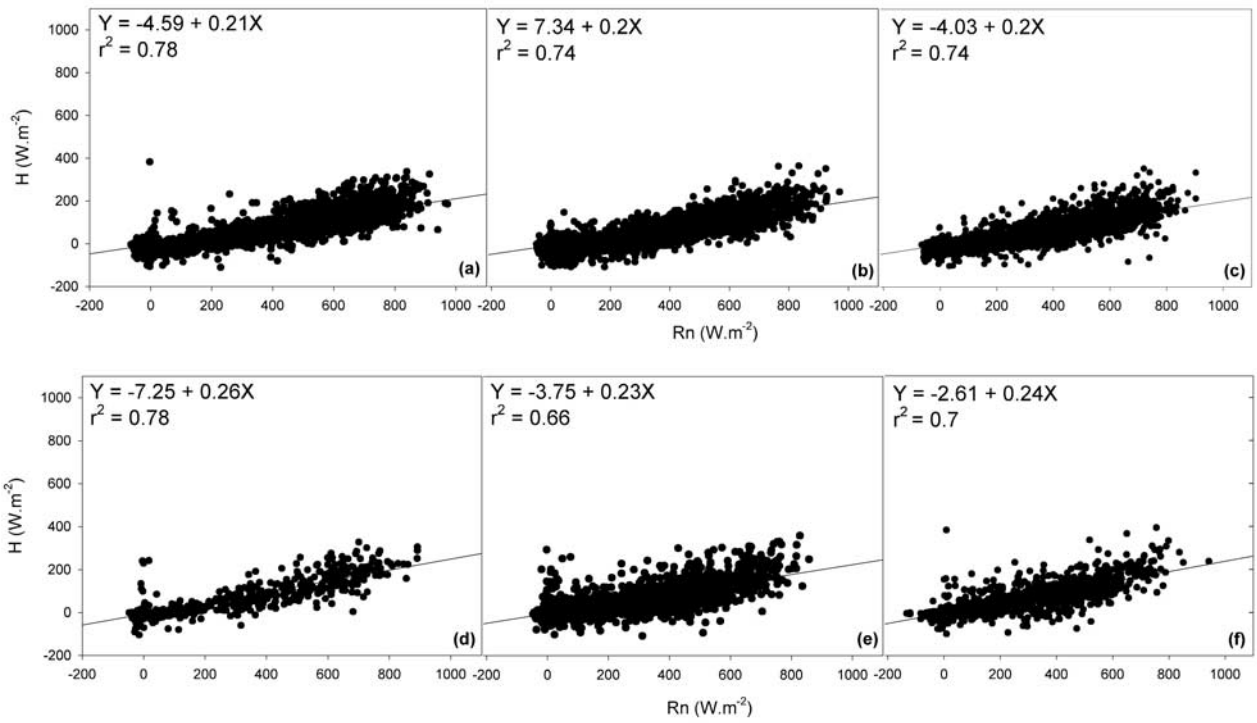

Figure 10. Net radiation partitioning into sensible heat flux (H) for different seasons: (a) K34 first dry season (mid-July until November 1999, n = 5510), (b) wet season (December 1999 until May 2000, n = 6990), and (c) second dry season (June until September 2000, n = 5054); (d)–(f) C14 for the same seasons (n = 1224; n = 4370, and n = 2601, respectively). Points for K34 are half-hourly averages and for C14 are hourly averages.

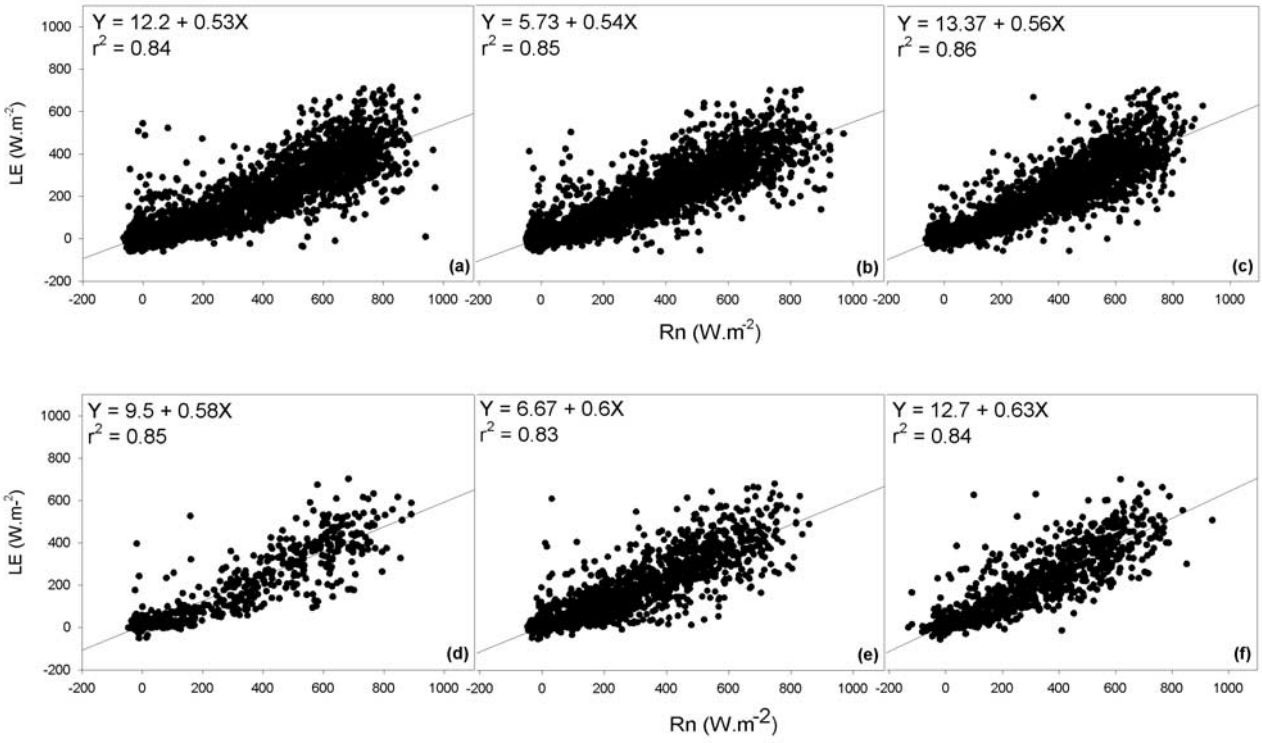

Figure 11. Net radiation partitioning into latent heat flux (LE) for different seasons: (a) K34 first dry season (mid-July until November 1999, n = 5510); (b) wet season (December 1999 until May 2000, n = 6990); and (c) second dry season (June until September 2000, n = 5054); (d)–(f) C14 for the same seasons (n = 1224; n = 4370, and n = 2601, respectively). Points for K34 are half-hourly averages and for C14 are hourly averages.

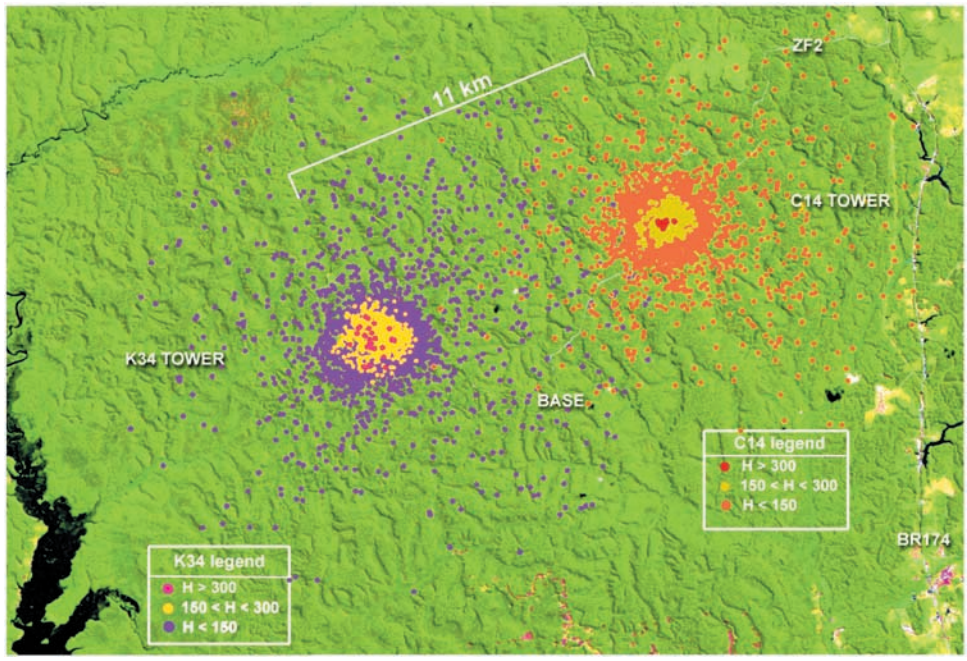

Figure 12. Estimate of tower flux sampling area (footprint) under unstable conditions (u* > 0.2 m s^{-1}) for the 1999/2000 period, plotted onto a Landsat TM image of the Cuieiras reserve. Fluxes were divided into three energy classes: H < 150 W m^{-2}; 150 < H < 300 W m^{-2}; and H > 300 W m^{-2}.

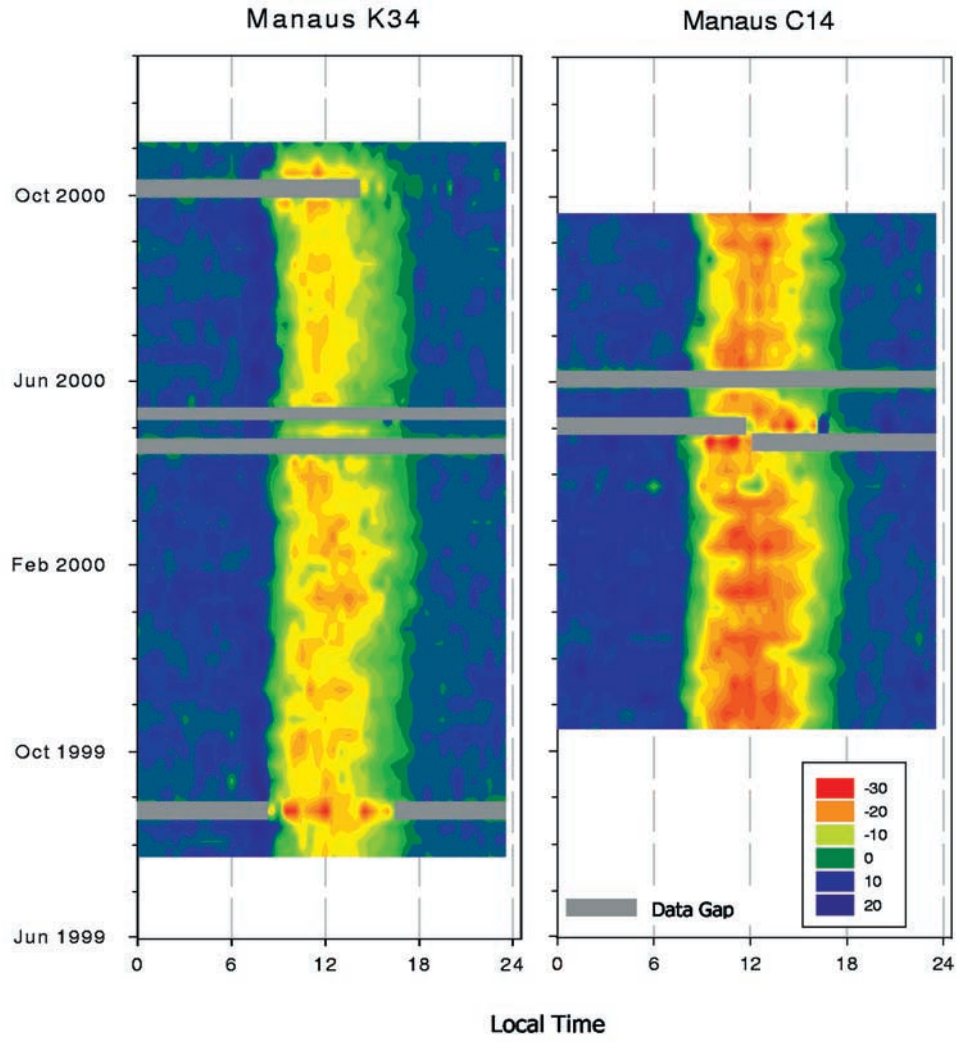

Figure 13. Contours of 10-day averages of daily course eddy flux CO_2 exchange for both towers. Entire data set plotted; missing data appear as gray areas.

the data sets. Purely statistical uncertainty bounds could be attached to this fit, amounting to about 5 kg C ha^{-2} d^{-1}.

[25] Clear differences between the towers appear in the intensities of the peak daytime sink strength and total daily NEE, which are higher for the C14 forest. This is surprising on first sight, because the two forest sites are only 11 km apart. The question immediately arises whether this is a real difference in canopy exchange rates or the result of some measurement artifact. Except for a lower measuring height and a longer sampling tube at C14, the instruments and methods used on both towers were identical, as were the data collection and analysis procedures, The difference in height is likely to affect the magnitude of frequency response correction functions. For a 10-day test period in October 1999, these corrections were typically -0.5 μmol m^{-2} s^{-1} for average daytime conditions and -1.7 μmol m^{-2} s^{-1} for the peak value. Decreasing measurement height and increasing tube length change these corrections by only a few tenths of units, indicating that the difference between towers is unlikely to be the result of measurement height or frequency response corrections applied [*Kruijt et al.*, 2002]. Therefore it is likely that we have measured real and significant physiological differences in rainforests 11 km apart. However, we are still conducting exhaustive instrument intercomparisons, using a third mobile system for extended periods on both towers, to eliminate uncertainties about potential instrumental differences (A. Manzi et al., manuscript in preparation).

[26] A possible ecological explanation for the difference in fluxes lies in the larger area with taller forest in C14 and, conversely, in the larger area of waterlogged vegetation in K34. The C14 plateau forest has older and taller individual trees than the K34 plateau forest, which could mean better access to deep soil water at C14. Also, a possible indication that waterlogged vegetation is less productive than upland forests came from the only published airborne regional transect study made so far in the Amazon by *Wofsy et al.* [1988], recording the CO_2 concentration diurnal cycle (resulting from nighttime emission and daytime consumption). In that study, over forests the lower atmosphere presented much stronger oscillations in concentration than over wetlands.

[27] Figure 15 shows monthly averaged diurnal cycles, for the three seasons in the present data set (1999 and 2000 dry seasons, 1999/2000 wet season) of above-canopy CO_2 flux for both towers along with radiation and air temper-

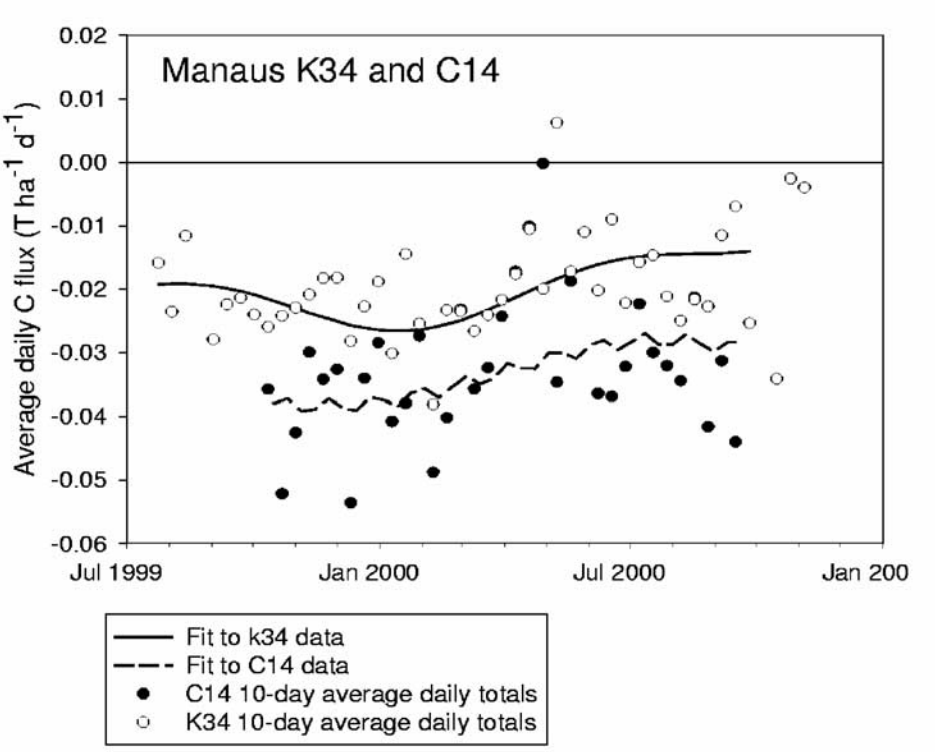

Figure 14. Variation over time of 10-daily average daily totals (not u*-filtered) and an empirical multiple sine fit to the full 30-min period-by-period variation in the data sets for both towers. The fitted function also yields a 95% confidence interval, giving an indication of the internal consistency of the data between 10-day periods.

ature for K34 only. Similarities in the shapes of this diurnal variation between the two forests indicate again that regional forcing is dominant, affecting both forests equally, independently from their peak photosynthetic capacities. The effect of La Niña on the 1999 dry season could explain the much higher peak in the response at C14 for October 1999. For this month cloud free days were followed by frequent thunderstorms in the evenings, therefore creating optimum conditions for photosynthesis (high availability of both photons and water). At the end of the wet season, April of 2000, water was abundant, but overcast days were frequent, with reduced light availability. Finally, for September of 2000, radiation was abundant, but water was missing. These results suggest that peak photosynthesis at C14 follows the limitations posed by the interplay of water and radiation better than that at K34. That difference in response could well indicate that K34 forest takes less advantage of extra environmental resources, like radiation and water, because a larger proportion of its trees either not reaching the groundwater or being limited by water logging. Despite the availability of potential physiological explanations for the difference between C14 and K34, a verifiable explanation for these differences would require more detailed research, such as explicit quantification of (leaf-scale) photosynthesis, in the forests within the footprint area for both towers, with accurate mapping of parameters like LAI, biomass and respiration.

4.4.2. Average Diurnal Variation and Nighttime Fluxes

[28] There is a distinct difference in the diurnal trends of days where the preceding night was calm, with little turbulent mixing and much accumulation of respired CO_2 inside the canopy, and where the night was windier, with sufficient mixing to minimize the amount of CO_2 stored inside the canopy. Figure 16 shows such diurnal trends, averaged for all 24 hour periods in the data set, where the average friction velocity (u*) above the canopy during the preceding night was either below 0.05 m s^{-1} or above 0.15 m s^{-1} (n = about 30 in each average). Both the above-canopy flux and the storage flux underneath the flux system are shown. These plots can be used to examine the consequences of the nighttime turbulence regime not only for night fluxes, but also for the build-up of fluxes during the following day. During the calm nights, the ''eddy flux'' is almost negligible, whereas storage accounts for about 3 μmol m^{-2} s^{-1}. During windier nights, storage is small and the eddy fluxes are around 5 μmol m^{-2} s^{-1}, sometimes peaking to more than double that value. Therefore the NEE, calculated as the sum of eddy flux and storage flux, is clearly depressed during calm nights. This is also illustrated by plotting half-hourly nighttime NEE values against above-canopy u_*, after *Goulden et al.* [1996], showing suppressed NEE values when u* drops below 0.2–0.3 m s^{-1} (Figure 17). Such a relationship is often observed for flux towers and used to correct nighttime ''losses'' by assuming NEE values derived from those occurring at higher u*. As in the case of the present data the vast majority of data points occurs at u* below 0.2 m s^{-1}, and the values do not show a clear plateau above this threshold, it is useful to critically assess whether the observed sup-

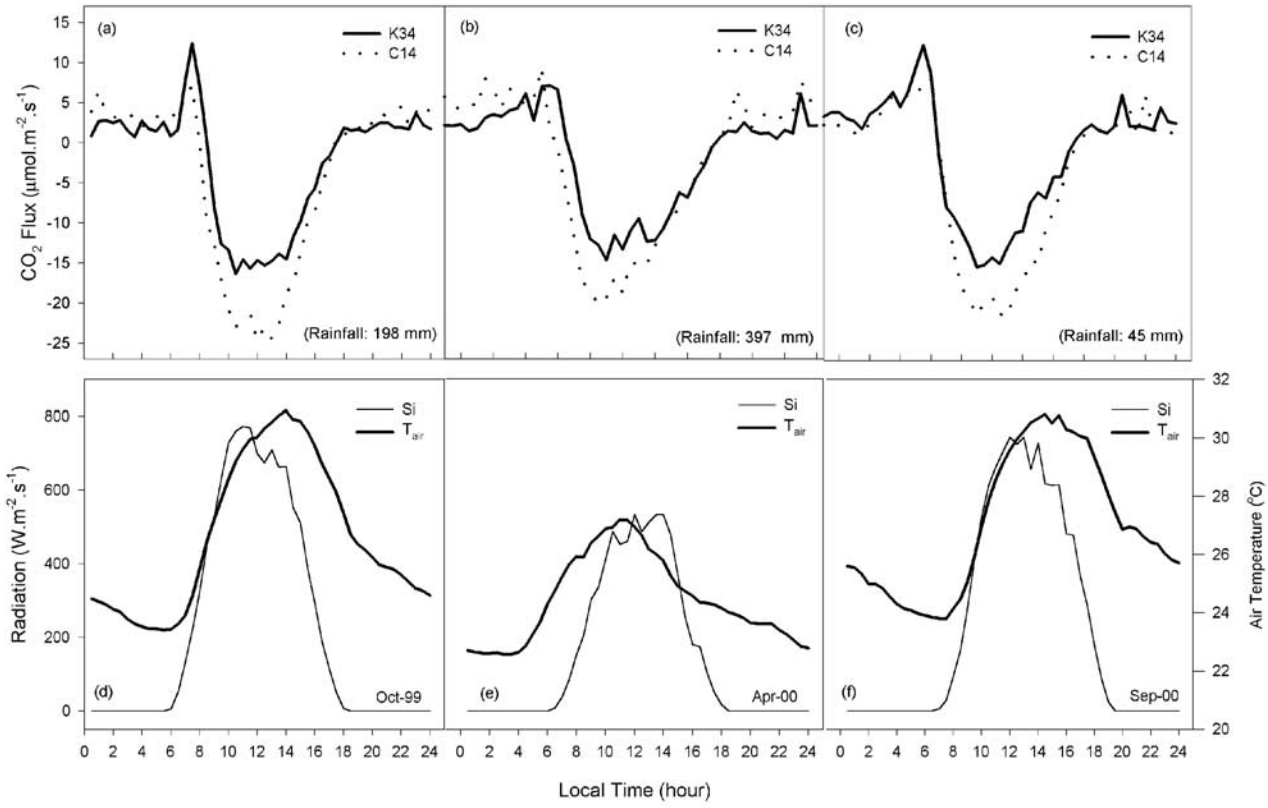

Figure 15. Mean diurnal cycle of the above-canopy carbon flux, solar incoming radiation and air temperature as they vary between wet and dry seasons for both towers: (a) and (d) on dry season (October 1999) with rainfall of 198 mm; (b) and (e) on wet season (April 2000) with rainfall of 397 mm; and (c) and (f) on dry season (September 2000) with rainfall of 45 mm. The solar incoming radiation and air temperature were measured at K34 tower only.

pression of NEE really represents an error to daily net carbon exchange.

[29] To study the effects of low nighttime turbulence more closely, thirteen nights were selected from the 1999 data set, when above canopy flux was large and storage close to zero for at least 2.5 h. The periods chosen and the average fluxes are given in Table 3. None of these periods exhibited a period of high emissions during the early daylight hours, associated with the onset of convective turbulence. During these nights the average flux measured above the canopy was 6.2 μmol m^{-2} s^{-1}. The range of values (2.8 to 10.4 μmol m^{-2} s^{-1}) was large, however. Then, nine nights were identified in 1999 during which the carbon dioxide flux measured at the top of the tower was close to zero for several consecutive hours. The build up of carbon dioxide below the flux measurement level during these periods was significantly greater than on nights when flux was observed, but only ranged from 2.9 to 5.6 μmol m^{-2} s^{-1}, with an average value of 4.1 μmol m^{-2} s^{-1} (Table 4). Nighttime storage measurements during calm nights do not match the eddy flux during windy nights.

[30] Further examining Figure 16, we can see that just after sunrise, after calm nights, there is often a peak in the upward flux of CO_2 which is attributed to the flushing out of the CO_2 stored overnight beneath and within the canopy. The peaks in above-canopy flux are then followed after 1.5 to 2 h, by a negative storage flux, caused by rapid decreases in canopy CO_2 concentrations. These peaks are almost absent after more windy nights, but after all nights there is a consistently negative but diminishing storage flux until the end of the following day's afternoon.

[31] If the diurnal courses of eddy flux and storage flux are followed further in Figure 16 it can also be seen that a substantial part of the nighttime flux difference between windy and calm nights is compensated for by an excess emission flux (positive NEE, or NEE responding less sharply to increasing radiation) in the morning. This points at additional CO_2 entering the storage laterally or from the soils. If the diurnal trends are integrated, however, the difference is not completely canceled at the end of these days. This means either that a residual quantity of flux is actually "lost," requiring a correction, or that other factors may explain the higher net uptake after calm nights, such as the fact that total incoming radiation (not shown here) was also higher during such periods.

[32] A recent intensive short-term study has found emissions of CO_2 from the soils in the Cuieiras reserve to range from 3.28 to 10.04 μmol m^{-2} s^{-1}, with an average efflux of 6.53 (±0.29) μmol m^{-2} s^{-1}, temperature of 25.9°C at 5 cm depth, values well within the range of previous measurements in the Amazon [*Sotta*, 1998]. The same study has also shown that soil water is an important controlling factor on

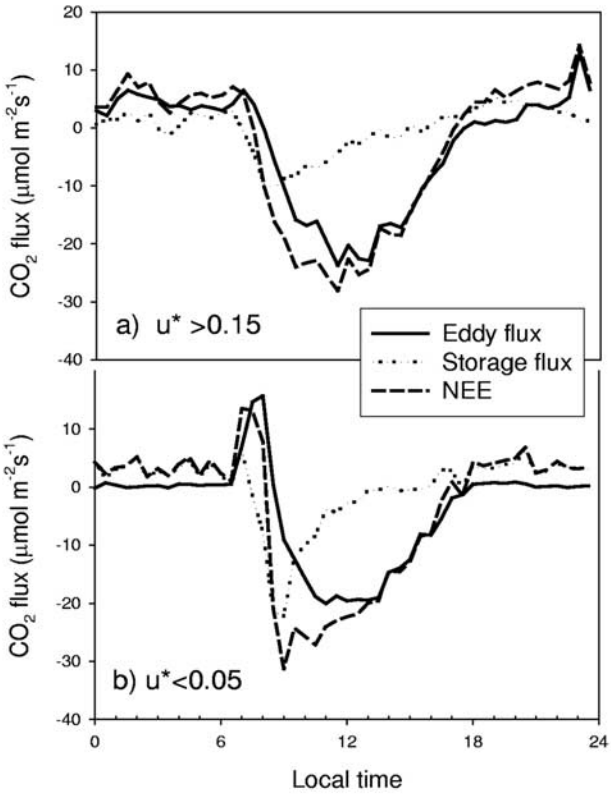

Figure 16. Average diurnal trend of eddy flux, storage flux and NEE for (a) windy and (b) calm nights.

efflux, especially in the dry season and during, and soon after, rainfall events. Even though temperature might play a smaller role in determining respiration variations under the relatively unchanging local climate in southwest Amazon, *Meir et al.* [1996] identified a relationship between soil respiration and soil temperature with a reasonable r^2 range of 0.76–0.88. Nighttime CO_2 efflux from above ground respiring wood and leaves was measured in SW Amazonia at 0.7 (±0.3) μmol m^{-2} s^{-1} and 1.0 (±0.1) μmol m^{-2} s^{-1}, respectively [*Meir et al.*, 1996]. More recently, *Chambers et al.* [2001b] measured coarse litter CO_2 efflux varying by almost two orders of magnitude (~0.014 to 1.003 μg C g^{-1} C min^{-1}) for the forest at K34.

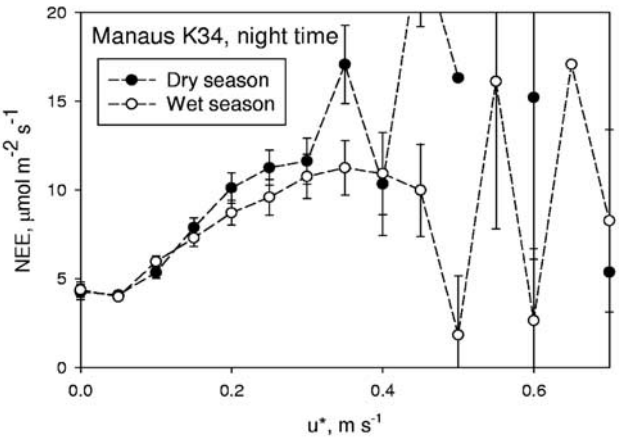

Figure 17. The average dependence of nighttime NEE on associated u* at K34, for dry and wet seasons.

Table 3. Measured Nocturnal Flux Over Periods With Zero Storage Below Flux Measurement Level

Night of 1999	Time Period, LT	Average Flux, μmol m^{-2} s^{-1}	Average u*, m s^{-1}
267–268	02:00–03:30	9.9	0.11
269–270	23:30–02:00	4.1	0.14
278–279	23:00–02:00	4.4	0.14
279–280	21:00–00:30	8.7	0.36
283–284	24:00–03:00	4.0	0.11
302–303	22:30–01:30	10.4	0.25
305–306	23:30–07:00	5.3	0.23
316–317	22:00–04:00	7.1	0.23
318–319	01:30–07:00	8.2	0.11
327–328	02:00–07:00	5.2	0.15
340–341	23:00–02:30	6.4	0.15
356–357	03:00–06:30	2.8	0.08
361–362	23:00–05:00	3.7	0.1

[33] Therefore measurements and modeling of tropical forest respiration give values close to 7 μmol m^{-2} s^{-1}, and the average flux during windy nights with low storage was only little less than this, suggesting that under these conditions the respirative flux is well captured by the eddy flux measurements. It appears likely, however, that in nights with low above-canopy flux the combination of flux measurement and storage profile does not capture the full respirative output of the forest, as suggested for other forests before, although the discrepancy is much smaller than has been observed at some other sites [*Goulden et al.*, 1996; *Aubinet et al.*, 2000]. Such discrepancy is often ascribed to downhill drainage of CO_2 during calm nights.

[34] The analysis of fluxes during the subsequent daytime hours, suggests, however, that apparent losses of CO_2 emissions in such conditions are recovered during the subsequent (later night or daytime) hours. Similar conclusions have also been drawn by other studies on the same sites [*Malhi et al.*, 1998] and by more recent and elaborate analysis of the present data sets [*Kruijt et al.*, 2002]. The source for this recovery of night losses has not been identified yet. It may be located for example in the topsoil, or be represented by elevated CO_2 welling up from the valley bottoms during early morning, where it may have been stored after nocturnal drainage from the slopes.

Table 4. Build-up of CO_2 Below the Flux Measurement Level During Periods When Measured Flux Was Close to Zero

Night of 1999	Time Period, LT	Average Flux Above Canopy, μmol m^{-2} s^{-1}	Average Rate of Build-Up Below Flux Measurement, μmol m^{-2} s^{-1}	Average u*, m s^{-1}
263–264	00:30–06:30	0.02	5.1	0.04
270–271	20:30–07:30	−0.01	3.4	0.02
275–276	23:30–06:00	−0.05	3.2	0.03
297–298	21:00–02:00	−0.02	2.9	0.03
299–300	17:30–22:00	−0.07	3.4	0.03
309–310	18:30–00:30	−0.05	3.7	0.02
328–329	21:30–06:00	−0.12	5.6	0.03
346–347	21:30–06:00	−0.04	3.0	0.02
362–363	20:00–23:30	0.06	5.0	0.02

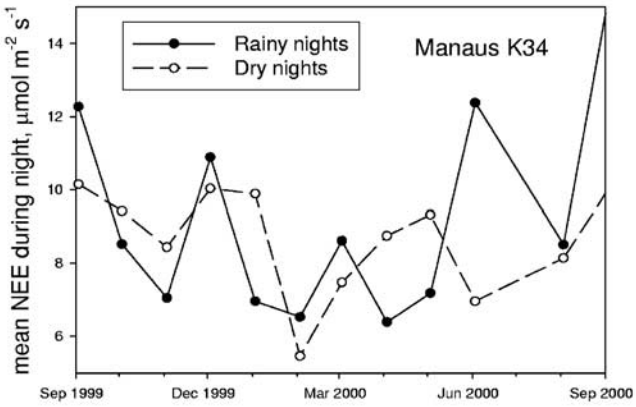

Figure 18. Average monthly nighttime NEE values for rainy and dry nights at K34.

[35] In any case, these analyses show that the exchange of CO_2 from the canopy space is still poorly understood. It may also be necessary to consider to what extent windy and calm nights and days are associated with different weather, different wind directions and footprint composition (A. Araújo et al., manuscript in preparation, 2001). It may be too early yet to accept that low CO_2 flux measurements during calm nights just represent a failing response of the measurement system [*Goulden et al.*, 1996], and need to be corrected.

[36] The nighttime NEE varied over time and between the two towers. Figure 18 shows the annual course of storage corrected night fluxes for K34, showing lower values during the wet season. The CO_2 profile was only monitored at K34 and for C14 storage was calculated using K34 profile data. Table 5 gives values for average nighttime fluxes during rainy and dry periods in both towers. Consistent with the observed seasonality, emissions appear slightly higher in the dry season, although the difference is not significant for C14. Again, the differences between sites can be ascribed to the larger area of waterlogged vegetation in K34 than in C14. As noted by *Sotta* [1998], water excess can impede CO_2 escape from the soil, but also it can generate anaerobic conditions favoring other respirative biochemical pathways that produce less CO_2 and more dissolved organics and other volatiles.

4.5. Net Ecosystem Carbon Exchange

[37] Although we do not fully understand the errors and uncertainties involved in eddy correlation CO_2 flux measurements at night, it is of interest to make preliminary estimates of the annual carbon balance for the sites. In principle, calculating the total net ecosystem carbon exchange is very simple. An addition over time of the above-canopy-measured fluxes is sufficient, with proper scaling to units of T ha^{-1} y^{-1}. In this case, storage fluxes do not have to be taken into account, since over timescales of days or longer, storage should integrate to zero, unless there are substantial permanent changes in canopy air CO_2 concentrations over such a time period.

[38] In practice, however, there are always data gaps and periods during which measured fluxes have to be rejected. In this case, unless the distribution of gaps is strictly random, these gaps need to be "filled" with representative values to avoid bias. Several methods to do this have been proposed, and they can be roughly subdivided into "empirical response functions" and "pure interpolation" [*Falge et al.*, 2001]. In the first case, during daytime usually an empirical, saturating light response function is used to estimate NEE. During nights, there is the additional complication of apparent losses during low turbulence events. If the choice is made to replace such data with an estimate of nighttime fluxes, different procedures can be adopted [*Aubinet et al.*, 2000]. A constant value can be estimated as the average of nighttime fluxes during higher turbulence events, or "fill" values could be allowed to vary according to time of year or other conditions. It is important to realize that in the case where nighttime gaps are filled with an estimate of the real efflux, the unaffected data should be storage corrected. If this is not the case, the risk is that "corrected" low-turbulence events are in fact already compensated for some time later in the data set, and sources are double-counted.

[39] In this study we adopted two approaches to estimate the annual carbon balance and the conceptual uncertainty in this. In the first, day-time gaps were always filled with a light response function fitted to the remaining data, but for the nights, data were either unaltered and simply integrated over time, or filtered for low-turbulence events (when friction velocity u* was lower than 0.2 m s^{-1}). These gaps, amounting to 89% (K34) and 86% (C14) of all nighttime data, ideally then should be filled with an estimate of nighttime flux dependent on day of year and on whether or not there was any rainfall during the night, as was shown in Figure 18 and Table 5. However, because of the high uncertainty in appropriate nighttime filling methods we chose to simply fill these nighttime gaps with a constant value of 5.4 µmol m^{-2} s^{-1} for K34 and 6.5 µmol m^{-2} s^{-1} for C14, representing the average measured nighttime NEE values for those sites. Again, C14 storage was calculated using K34 profile data.

[40] Figure 19 shows the cumulative balance of carbon over time for both towers, for both nonfiltered and (simply) filtered data treatments. It is clear that the choice whether or not to filter and replace nighttime data represents the single major uncertainty in the whole estimation process. The choice can turn a very large carbon sink into a moderate one or even into a small source. At present, it is yet unclear how to deal with nighttime losses of flux, although in the preceding analysis we suggest that simple rejection of calm nighttime data might be as unjustified as simply keeping it unfiltered. As expected, the cumulative uptake is larger for the C14 site than for K34, and again it remains to some extent uncertain whether this difference is real or the result of differences in the measurements.

Table 5. Average Nighttime NEE During the 1999/2000 Period for K34 and C14[a]

	Rainy Nights	Dry Nights
K34	8.15 (0.10)	8.56 (0.05)
C14	9.54 (0.04)	9.57 (0.07)

[a] Fluxes were classified according to absence or presence of rainfall and selected for friction velocity above 0.2 m s−1. Values in parentheses are standard errors of the means.

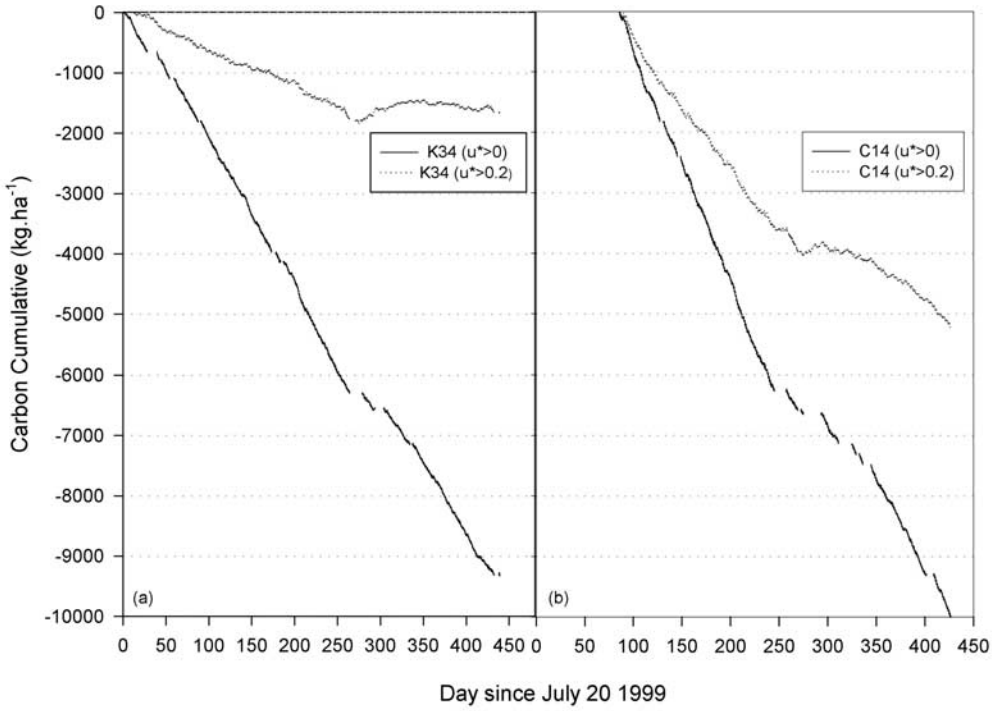

Figure 19. Cumulative balance of carbon over time calculated with or without gap filling for low friction velocities (u* < 0.2).

[41] Finally, a word of caution. So far this study has only represented the results and analysis of our observations, and of a critical assessment of assumptions that are often made about missed emissions at night. The observations, on one extreme, lead to very high uptake rates. Very roughly, such rates, if sustained over many decades, would imply a doubling of forest biomass and soil carbon in 15–20 years, which is clearly not possible [*Chambers et al.*, 2001a]. Also, if such high uptake rates would apply for the whole Amazon forest biome, they would be in contrast with most global atmospheric inversion studies, which after correction for anthropogenic and deforestation emissions, point to an average uptake rate of order only 1 T ha^{-1} y^{-1} [*Malhi and Grace*, 2000]. However, *Wofsy et al.* [1988], in a regional atmospheric budget study, suggested that although the atmosphere over the Amazon as a whole did not seem to be depleted in CO_2, implying zero net carbon uptake, this may well reflect the balance of substantial uptake in terra firma areas and release in low-lying wetlands. In conclusion, it remains to be proven that the high uptake rates measured by eddy correlation are representative for the forest. Further work will have to evaluate to what extent this phenomenon could be part of an ENSO-dependent cycle, an effect of disturbance, or that substantial lateral leakage of carbon to the rivers occurs.

5. Concluding Remarks

[42] The Manaus LBA site is the first in the tropics with two eddy flux towers close to each other monitoring the same type of land use. If on further testing the instrumentation of the two towers proves indeed comparable, as we expect it to be, it is possible that we have identified real differences in ecosystem physiology. Testing these differences independently will require extended ecological characterization and measurements for both sites. Ongoing LBA research projects studying the K34 catchment aim at understanding the underlying ecological factors associated with a potential sustained sink. New similar studies need to be extended to the C14 catchment, as well as to other LBA sites in different ecoregions. Because the Amazon rainforest by and large is composed of a patchy and complex mosaic of upland vegetation intermingled with drainage-associated waterlogged vegetation, being able to discriminate their respective ecosystem responses would be of great value for a better estimation and modeling of the carbon balance in wider areas.

[43] **Acknowledgments.** This research was part of EUSTACH-LBA, a project funded by the European Commission grant ENV4-CT97-0566. We are grateful to A. Cruz, H. Xavier, V. Souza, and A. C. Lessa for invaluable field and logistic support, as well as the general support of INPA. We would particularly like to thank Flavio Luizão, Manaus LBA leader; Ari Marques, head of INPA projects office; INPE and the central LBA office, essential in the administration of funds and supply of vehicle; Alterra and Maarten Waterloo for coordination and scientific support; Johannes A. Dolman for his enthusiastic inspiration in the beginning of this study; and Carlos Nobre for his successful strategic vision in the leadership of LBA. Data are available on the Beija Flor metadata LBA Data Information System at http://beija-flor.ornl.gov/lba/.

References

Andreae, M. O., et al., Biogeochemical cycling of carbon, water, energy, trace gases and aerosols in Amazonia: The LBA-EUSTACH experiments, *J. Geophys. Res.*, *107*, 8066, doi:10.1029/2001JD000524, 2002.

Araújo, A. C., et al., Manaus rainforest in the LBA: Physical, ecological and land use characterization of the site, paper presented at First LBA Scientific Conference, Belém, Pará, Brazil, 26–30 June, 2000.

Aubinet, M., et al., Estimates of the annual net carbon and water exchange of forests: The EUROFLUX methodology, *Adv. Ecol. Res.*, *30*, 113–175, 2000.

Chambers, J. Q., N. Higuchi, E. S. Tribuzy, and S. E. Trumbore, Sink for a century: Carbon sequestration in the Amazon, *Nature*, *410*, 429, 2001a.

Chambers, J. Q., J. P. Schimel, and A. D. Nobre, Respiration from coarse wood litter in central Amazon forests, *Biogeochemistry*, *52*, 115–131, 2001b.

Culf, A. D., G. Fisch, and M. G. Hodnett, The albedo of Amazonian forest and ranch land, *J. Clim.*, *8*, 1543–1554, 1995.

Culf, A. D., G. Fisch, Y. Malhi, R. C. Costa, A. D. Nobre, A. O. Marques Filho, J. H. C. Gash, and J. Grace, Carbon dioxide measurements in the nocturnal boundary layer over Amazonian forest, *Hydrol. Earth Syst. Sci.*, *3*(1), 39–53, 1999.

Culf, A. D., A. D. Nobre, J. Elbers, A. C. Araújo, and P. Stefani, Energy and carbon fluxes at the Manaus K34 site: Instrument performance and error analysis, paper presented at First LBA Scientific Conference, Belém, Pará, Brazil, 26–30 June, 2000.

Dallarosa, R. L. G., and R. T. Clarke, Uma comparação entre diferentes estimativas da condutância superficial numa floresta primária na Amazônia central, *Acta Amazonica*, *30*, 291–304, 2000.

Elbers, J. A., Eddy correlation system Winand Staring Centre, user manual version 2.0, internal report, pp. 1–38, DLO-Staring Centre, Wageningen, Netherlands, 1998.

Falge, E., et al., Gap filling strategies for defensible annual sums of net ecosystem exchange, *Agric. For. Meteorol.*, *107*, 71–77, 2001.

Fan, S.-M., S. C. Wofsy, P. S. Bakwin, and D. J. Jacob, Atmosphere-biosphere exchange of CO_2 and O_3 in the central Amazon forest, *J. Geophys. Res.*, *95*, 16,851–16,864, 1990.

Fisch, G., J. A. Marengo, and C. A. Nobre, Uma revisão geral sobre o clima da Amazônia, *Acta Amazonica*, *28*, 101–126, 1998.

Fitzjarrald, D. R., K. E. Moore, O. M. R. Cabral, J. Scolar, A. O. Manzi, and L. D. A. Sa, Daytime turbulent exchange between the Amazon Forest and the atmosphere, *J. Geophys. Res.*, *95*, 16,825–16,838, 1990.

Grace, J., et al., Carbon dioxide uptake by an undisturbed tropical rainforest in southwest Amazonia, 1992 to 1993, *Science*, *270*, 778–780, 1995.

Grelle, A., and A. Lindroth, Eddy-correlation system for long-term monitoring of fluxes of heat, water vapour and CO_2, *Global Change Biol.*, *2*, 297–307, 1996.

Goulden, M. L., J. W. Munger, S.-M. Fan, B. C. Daube, and S. C. Wofsy, Measurements of carbon sequestration by long-term eddy covariance: Methods and a critical evaluation of accuracy, *Global Change Biol.*, *2*, 169–182, 1996.

Higuchi, N., J. Santos, R. J. Ribeiro, J. V. Freitas, G. Vieira, A. Coic, and L. J. Minette, Crescimento e incremento de uma floresta Amazonica de terra-firme manejada experimentalmente, in *Biomassa e Nutrientes Florestais*, *BIONTE*, *Relatorio Final*, pp. 89–132, Inst. Nac. de Pesquisas da Amazônia, Manaus, Brazil, 1997.

Jardim, F. C. S., and R. T. Hosokawa, Estrutura da floresta equatorial úmida da estação experimental de silvicultura tropical do INPA, *Acta Amazonica*, *16/17*, 411–508, 1987.

Kruijt, B., Y. Malhi, J. Lloyd, A. D. Nobre, A. Culf, A. C. Miranda, M. G. P. Pereira, and J. Grace, Turbulence above and within two Amazon rainforest canopies, *Boundary Layer Meteorol.*, *94*, 297–311, 2000.

Kruijt, B., J. Elbers, C. von Randow, A. C. Araujo, A. Culf, N. J. Bink, P. J. Oliveira, A. O. Manzi, A. D. Nobre, and P. Kabat, Aspects of the robustness in eddy correlation fluxes for Amazon rainforest conditions, *Ecol. Appl.*, in press, 2002.

Malhi, Y., and J. Grace, Tropical forests and atmospheric carbon dioxide, *Trends Ecol. Evol.*, *15*, 332–337, 2000.

Malhi, Y., A. D. Nobre, J. Grace, B. Kruijt, M. G. P. Pereira, A. Culf, and S. Scott, Carbon dioxide transfer over a central Amazonian rainforest, *J. Geophys. Res.*, *103*, 31,593–31,612, 1998.

Malhi, Y., E. Pegoraro, A. D. Nobre, M. G. P. Pereira, J. Grace, A. Culf, and R. Clement, Energy and water dynamics of a central Amazonian rainforest, *J. Geophys. Res.*, *107*, doi:10.1029/2001JD000623, in press, 2002.

McMillen, R. T., An eddy correlation technique with extended applicability to non-simple terrain, *Boundary Layer Meteorol.*, *59*, 279–311, 1988.

Meir, P., J. Grace, A. Miranda, and J. Lloyd, Soil respiration in a rainforest in Amazonia and in Cerrado in central Brazil, in *Amazonian Deforestation and Climate*, edited by J. H. Gash et al., pp. 319–329, John Wiley, New York, 1996.

Moncrieff, J. B., J. M. Massheder, H. de Bruin, J. Elbers, T. Friborg, B. Heusinkveld, P. Kabat, S. Scott, H. Soegaard, and A. Verhoef, A system to measure surface fluxes of momentum, sensible heat, water vapour and carbon dioxide, *J. Hydrol.*, *188–189*, 589–611, 1997.

Moore, C. J., Frequency response corrections for eddy correlation systems, *Boundary Layer Meteorol.*, *37*, 17–35, 1986.

Nelson, B. W., V. Kapos, J. B. Adams, W. J. Oliveira, O. P. G. Braun, and I. L. do Amaral, Forest disturbance by large blow downs in the Brazilian Amazon, *Ecology*, *75*(3), 853–858, 1994.

Nobre, A. D., et al., Multiyear comparative analysis of NEP and environmental factors for Manaus rainforest: "La Niña" influence on CO_2 uptake, paper presented at First LBA Scientific Conference, Belém, Pará, Brazil, 26–30 June, 2000.

Schuepp, P. H., M. Y. Leclerc, J. L. Macpherson, and R. L. Desjardins, Footprint prediction of scalar fluxes from analytical solutions of the diffusion equations, *Boundary Layer Meteorol.*, *50*, 355–373, 1990.

Sotta, E. D., Fluxo de CO_2 entre solo e atmosfera em floresta tropical úmida da Amazônia central, M.S., thesis, Inst. Nac. de Pesquisas da Amazônia, Manaus, Brazil, 1998.

Tuomisto, H., K. Ruokolainen, R. Kalliola, A. Linna, W. Danjoy, and Z. Rodrigues, Dissecting Amazonian biodiversity, *Science*, *269*, 63–66, 1995.

Wofsy, S. C., R. C. Harris, and W. A. Kaplan, Carbon dioxide in the atmosphere over the Amazon basin, *J. Geophys. Res.*, *93*, 1377–1387, 1988.

A. C. Araújo, R. Dallarosa, and A. D. Nobre, Instituto Nacional de Pesquisas da Amazônia, Projeto LBA, Av. André Araújo, 2936 Manaus, AM, 69083-000, Brazil. (carioca@inpa.gov.br; dalla@inpa.gov.br; anobre27@yahoo.com)

A. D. Culf and J. H. C. Gash, Centre for Ecology and Hydrology, Maclean Building, Crowmarsh Gifford, Wallingford, Oxfordshire OX10 8BB, UK. (aculf@hotmail.com; jhg@ceh.ac.uk)

J. A. Elbers, P. Kabat, and B. Kruijt, Alterra, P.O. Box 47, 6700AA Wageningen, Netherlands. (j.a.elbers@alterra.wag-ur.nl; p.kabat@alterra.wag-ur.nl; b.kruijt@alterra.wag-ur.nl)

A. O. Manzi and C. von Randow, Instituto Nacional de Pesquisas Espaciais, CPTEC, Rodovia Presidente Dutra, Km 39, Cachoeira Paulista, SP 12630-000, Brazil. (manzi@cptec.inpe.br; randow@cptec.inpe.br)

P. Stefani and R. Valentini, Università degli Studi della Tuscia, Facoltà di Agraria, Dipartimento DI.S.A.F.RI, Via de Lellis snc., I-01100 Viterbo, Italia. (pstefani@unitus.it; rik@unitus.it)